



OPTIMISING COLLECTOR PLATE GEOMETRY FOR A SPECIFIC SOLAR SYPHON SYSTEM DESIGN

By

ALI MOHAMED ELHABISHI

Thesis submitted in fulfilment of the requirements for the degree

Master of Technology: Mechanical Engineering

in the Faculty of Engineering at the

Cape Peninsula University of Technology

Supervisor: Prof. J. Gryzagoridis

Bellville campus

April 2016

CPUT copyright information

The dissertation/thesis may not be published either in part (in scholarly, scientific or technical journals), or as a whole (as a monograph), unless permission has been obtained from the University.

DECLARATION

I, Ali Mohamed Elhabishi declare that the contents of this thesis represent my own unaided work, and that the thesis has not previously been submitted for academic examination towards any qualification. Furthermore, it represents my own opinions and not necessarily those of the Cape Peninsula University of Technology.

Signed

Date

ACKNOWLEDGEMENTS

I wish to thank and express my gratitude to Prof Jasson Gryzagoridis for his supervision of this thesis. I wish to thank him for all his advice, counselling, support, guidance and constructive criticism which helped to accomplish this work.

I also wish to thank the staff of the Mechanical Engineering Workshop for their assistance.

Special thanks to my colleagues (postgraduate students) whom I have had the pleasure of knowing, have had discussions with and shared knowledge.

Great thanks for all my family members

DEDICATION

This thesis is dedicated to my loved ones, with a special feeling of gratitude to my loving mother and sisters, who have been a constant source of support and encouragement during the challenges of graduate school and life. To my wife who has always loved me unconditionally and whom I am truly thankful. Finally, to my wonderful daughters and sons for being there for me throughout the entire master's program. You have all been my best cheerleaders.

Thank you!!

ABSTRACT

Solar energy is still not being used effectively in countries in the developing world, though it's a partial solution to the problem of shortage and expensive energy. Normally harvested through flat plate collectors, converting solar radiation into heat is the most direct application that can be effected in water heating systems. Many researchers have attempted to develop means of improving the efficiency of the flat plate solar energy collector; however there appears to be no evidence of any work regarding the effect of geometric configuration on the performance of flat plate solar collector.

This study presents results obtained when comparing the performance of a solar water heating system equipped with three manufactured flat plate solar collector panels of numerically identical surface area but of different geometric configuration as they were individually attached to a typical geyser. Data was obtained inside a laboratory. The amount of heat acquired from flat plate collectors of solar energy depends primarily on their surface area that is exposed to the solar irradiance, however, the geometry of the collectors was thought that it might affect to some extent the amount of heat harvested. The circulation of the water from the panel to the geyser was due to the self-induced thermo-syphon effect. The results obtained during the test period (7 hours per day for two consecutive days) indicated that the system's thermal efficiency was best when the square geometrical configuration collector was used. A dimensional analysis using the Π Buckingham method that was performed on the parameters affecting a flat plate solar collector yielded three dimensionless numbers that lead to a power law relationship which might be useful in enhancing solar water heating systems' design.

TABLE OF CONTENTS

DECLARATION	i
ACKNOWLEDGEMENTS	ii
DEDICATION.....	iii
ABSTRACT.....	iv
TABLE OF CONTENTS	v
LIST OF FIGURES	viii
LIST OF TABLES.....	x
Nomenclature	xi
CHAPTER ONE: INTRODUCTION	1
1.1 General background.....	1
1.1.1 The energy crisis.....	1
1.1.2 Historical overview of solar energy	1
1.1.3 The sun	5
1.2 Problem statement	5
1.3. Parameters that affect solar flat plate collector	6
1.3.1 Climatic parameters.....	6
The intensity of solar radiation	6
Dust.....	6
Shading.....	6
Wind.....	6
1.3.2 Design parameters	6
Plate.....	6
Glazing.....	7
Tube spacing.....	7
Tilt angle.....	7
1.4. Project objectives	7
1.5. Significance of the thesis.....	8
1.6. Limitations of the thesis	8
1.7. Organization of the thesis.....	8
CHAPTER TWO: THEORETICAL BACKGROUND	10
2.1 Solar energy.....	10
2.2 Heat Transfer	12

2.2.1	Conduction	12
2.2.2	Convection.....	12
2.2.3	Radiation.....	13
2.3	Important equations to calculate the solar water heating system's efficiency and acquired energy.	13
2.3.1	Energy input to the collector	14
2.3.2	Energy acquired by the geyser.....	14
2.3.3	Solar water heating system's efficiency.....	14
2.4	Dimensional analysis	15
2.4.1	Finding a functional relationship between variables by the Buckingham Π Method	15
2.4.2	Finding or calculating the difference in pressure between the inlet and outlet of the flat plate solar energy collector	17
CHAPTER THREE: THE METHODOLOGY OF THE EXPERIMENTS.....		20
3.1	Description of the thermo-syphon system	20
3.1.1	Geyser.....	24
3.1.2	Flat plate collectors	25
3.1.3	The sun simulator	26
3.1.4	Equipment holder or stand.....	28
3.1.5	Pipe connections	28
3.2	Instrumentation and experimental protocol	29
3.2.1	Laboratory's condition.....	29
3.2.2	Sun Simulator's radiation intensity measurement	29
3.2.3	Temperature measurements	30
3.2.4	Experimental Protocol.....	30
CHAPTER FOUR: RESULTS AND DISCUSSION.....		32
4.1	Introduction	32
4.2.	The test results for the water temperature inside the geyser during the:	32
	First day	32
	Second day.....	34
4.3	Energy acquired by the water in the geyser	36
	First day	36
	Second day.....	38

4.4	Thermo-syphon solar water heating system's efficiency	40
	First day	40
	Second day.....	41
4.5	Results from the dimensional analysis.....	41
CHAPTER FIVE: Conclusions and Recommendations		45
5.1	Conclusions.....	45
5.1.1	Results from the first day of the tests	45
5.1.2	Results from the second day of the tests	45
5.3	Recommendations for future work	46
REFERENCES		47
APPENDICES.....		50

LIST OF FIGURES

Figure 1.1: A solar bonfire by F. Marion, Hachette, Paris, 1876.....	2
Figure 1.2: The first solar furnace with glass concentrating lenses, built by F. Lavoisier.....	3
Figure 1.3: The solar engine water pump in California and the Shuman Bays solar power erected in Egypt.....	3
Figure 1.4: Shuman's flat plate collector sun power system.....	4
Figure 2.1: Schematic representation of solar radiation on Earth.....	10
Figure 2.2: Schematic of the heat balance on a flat plate solar radiation collector.....	11
Figure 2.3: Schematic diagram of the calculation of the static pressure difference across inlet and outlet of the flat plate solar energy collector.....	18
Figure 3.1: Schematic diagram of the thermos-syphon system.....	21
Figure 3.2a: The sun simulator positioned above the solar collector.....	22
Figure 3.2b: The geyser's various connections.....	23
Figure 3.3: Xstream Solar Hot Water geyser.....	24
Figure 3.4: The three flat plate collectors.....	26
Figure 3.5: The sun simulator.....	27
Figure 3.6: Equipment holder or stand.....	28
Figure 3.7: Solar Power meter (TES-1333).....	29
Figure 3.8: Testo 926 device and T-type thermocouples.....	30
Figure 4.1: Temperature variation of the water inside the geyser in the first day of the test for flat plate collector A.....	33
Figure 4.2: Comparison between average temperatures of the water in the geyser when using the flat plate collectors, A, B, and C (first day).....	34
Figure 4.3: The temperature variation of the water inside the geyser during the second day of the test when using collector A.....	35
Figure 4.4: Comparison between average temperature of the water in the geyser when using collectors A, B, and C in the second day.....	36
Figure 4.5: Comparison between the rates of energy acquired by the geyser's water using collectors A, B, and C relative to available irradiance during the first day of testing.....	37
Figure 4.6: Comparison of cumulative energy delivered to the geyser from the flat plate solar collectors A, B, and C during the first day.....	38

Figure 4.7: Comparison between energy acquired by the geyser’s water using collectors A, B, and C relative to available irradiance during the second day of testing.....	39
Figure 4.8: Comparison of cumulative energy delivered to the geyser from the flat plate solar collectors A, B, and C during the second day.....	39
Figure 4.9: Hourly efficiency of the flat plate solar collectors A, B and C during the first day of the tests.....	40
Figure 4.10: Hourly efficiency of the flat plate solar collectors A, B and C during the second day of the tests.....	41
Figure 4.11: The relationship between Π_3 and Π_2	42
Figure 4.12: The relationship between Π_2 and Π_3	43
Figure 4.13: The difference in pressure between the inlet and outlet of the inclined solar collector panel vs. the vertical height between them.....	44
Figure A-1: Variable voltage transformer-Variac model: SB-10 and specifications.....	49

LIST OF TABLES

Table 3.1: The specifications of the geyser.....	24
Table 3.2: The specifications of the flat plate solar collectors.....	25
Table 4.1: Shows the values of Π_1 , Π_2 and Π_3 ; and the average pressure difference on the collectors A, B and C based on their vertical height.....	42
Table A-1: Specification of Variable voltage transformer-Variac model: SB-10 and specifications.....	51
Table A-2: Solar power meter (TES-1333) specifications.....	52
Table B-1: Temperatures inside the geyser (in different locations) during the test period of the first day using collectors A, B, and C	56
Table B-2: Temperatures inside the geyser (in different locations) during the test period of the second day using collectors A, B, and C and C	57
Table D-1: T_{avg} , ΔT , energy rate acquired by the geyser's water (W), energy accumulated by the geyser's water (MJ) and hourly efficiency (%) were calculated during the test period of the first day using the collectors A, B, and C.....	62
Table D-2: T_{avg} , ΔT , Energy rate acquired by the geyser's water (W), Energy accumulated by the geyser's water (MJ) and Hourly efficiency (%) were calculated during the test period of the second day using the collectors A, B, and C.....	63
Table E: Temperature data, density values, enthalpy, pressure difference between the inlet and outlet of the flat plate collectors A, B and C and (Π_1 , Π_2 and Π_3).....	64

Nomenclature

Symbols	Description	Unit
A	Area	m ²
C _p	Specific heat	<i>kJ/kg.K</i>
g	Earth's gravity	m/s ²
H	water's specific enthalpy	Joules/kg
I	Solar radiation intensity	W/m ²
K	Thermal conductivity	W/mK
L	vertical height difference between input and output of the collector	m
M	Mass	Kg
P ₀	Atmospheric pressure	Pa
P _A	Inlet Pressure of the collector	Pa
P _B	Outlet Pressure of the collector	Pa
Δp	pressure difference between inlet and outlet of the flat plate solar energy collector	Pa
Q	Heat energy	<i>kJ</i>
T	Temperature	°C
t	Time	<i>hours</i>
ΔT	Temperature difference based on hourly data acquisition interval	°C
X	vertical dimensions in figure 2.3	m

Greek symbols	Description	Unit
α	Absorptance	-
τ	Transmittance	-
ε	Emissivity	-
σ	Stefan-Boltzmann constant	W/m ² K ⁴
η	Solar thermo-syphon system efficiency	%
ρ	Water density	kg/m ³
Π	Symbol for Dimensionless number	-

Chapter One

Introduction

1.1 General background

1.1.1 The energy crisis

Mankind in recent decades is experiencing continuous development in all fields, whether urban or industrial, and this development depends on the sources of energy. In most cases energy is derived from fuels such as coal, oil and gas, which are costly pollute the environment and will eventually be depleted. Solar energy is one of the solutions to help solve the energy problems in the world. Moreover, it is available over large areas on the earth and it is easy to be used. Most developed countries have been seeking to reduce the pressure on traditional energy sources and replace them with renewable energy [1].

The oil crisis started in the seventies of the last century when the war between Arabs and Israel threatened the oil supply lines. Many countries reviewed their plans of energy consumption and diversified their sources. Some countries opted for nuclear energy such as France and Sweden, and some turned their attention to alternative energy sources such as solar and wind energy [2].

In the last decade, South Africa has faced problems in the production of energy and it will also suffer a shortage of coal by this decade; a fuel the country needs for most of its power plants to produce electricity [3].

1.1.2 Historical overview of solar energy

Solar energy is the oldest type of natural energy used by humans. It provides the most basic needs for human beings such as light and warmth. It also plays a role in the climate and environmental cycle. In the present era, solar energy is considered to be the best solution to solve energy problems that are affecting the world [4]. Since ancient times humans benefited from solar radiation energy directly in many applications such as drying agricultural crops, drying meat and fish, and heating of homes etc. The Greek historian Plutarch (AD 46 – 120) pointed that Archimedes had used solar radiation to burn Roman ships in 212 BC by focusing solar radiation on them using hundreds of metal armour. Kircher (1601 – 1680) tried to prove whether this incident of Archimedes is true or not, so he conducted a scientific experiment by igniting wood using solar radiation from a distance.

Surprisingly, among the first applications of solar energy was using a concentrating collector (that requires accuracy in the construction and in tracking the sun) to start a solar bonfire. Figure (1) shows one of the first concentrating solar collectors

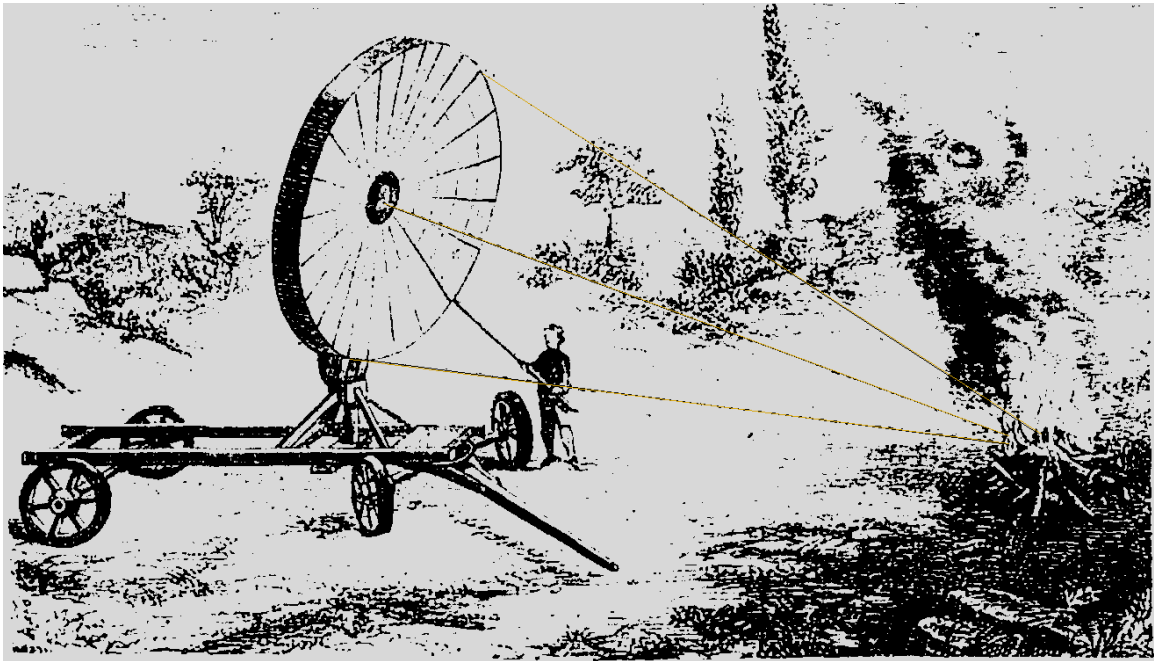


Figure 1.1: A solar bonfire by F. Marion, Hachette, Paris, 1876

(Adopted from [4])

The French scientist Antoine Lavoisier in the 18th century managed to design solar furnaces to melt metals reaching temperatures up to 1750 C by using lenses, as shown in figure (2). A collector (cone-shaped) was designed by Mouchot in 1895 in Algeria, which consisted of silver-plated metal plates, had a diameter of 5.4 m and a collecting area of 18.6 m². In the same period Abel Pifre designed a solar collector in a parabolic shape made of very small reflective mirrors. In 1901 a station was built to pump water in California using solar energy, as shown in figure (1.3a). The largest water pumping station operated by solar energy was built in Egypt in 1912, shown in figure (1.3b) [4],[5].

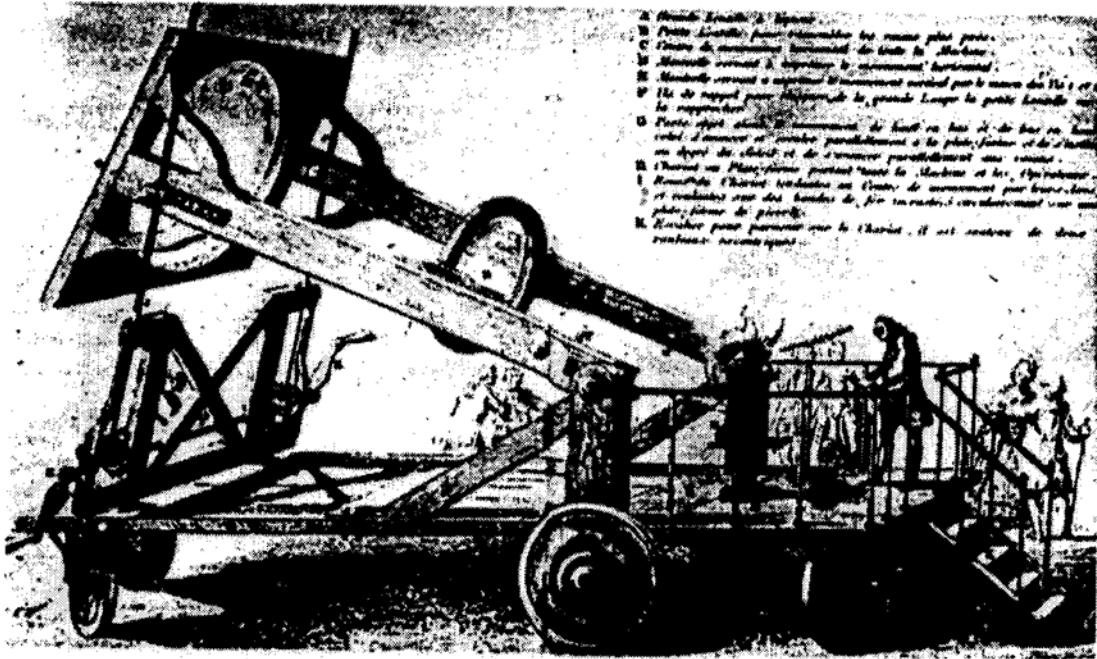


Figure 1.2: The first solar furnace with glass concentrating lenses, built by F. Lavoisier
 (Adopted from [4])

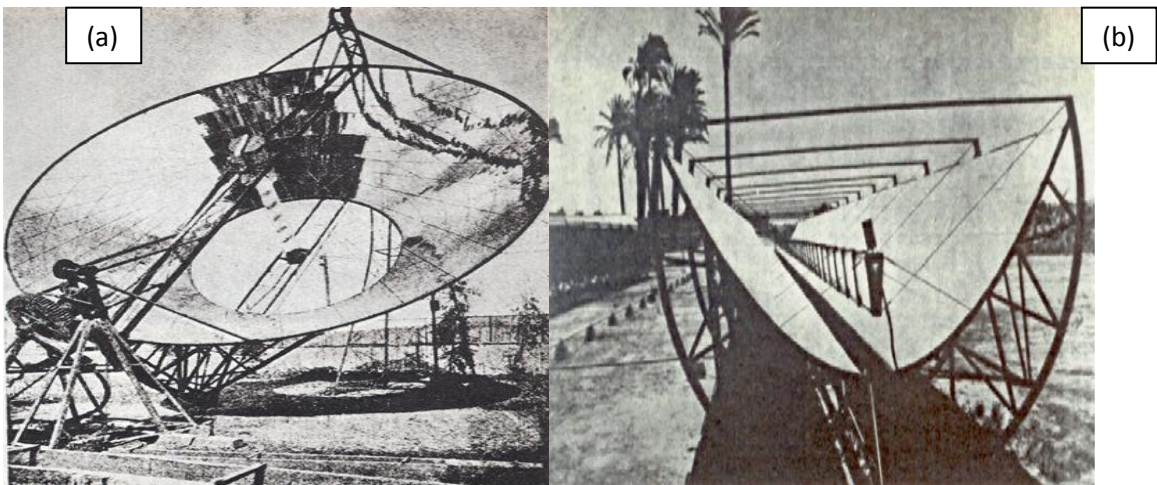


Figure 1.3: (a) The solar engine water pump in California, (b) the Shuman Bays solar power
 erected in Egypt
 (Adopted from [5])

One of the first designs of solar collectors used to heat water was by the Swiss scientist Horace de Saussure in 1760s. It was an isolated rectangular box shape, covered by glass [2]. In 1885 C.L.A. Tellier used the first flat-plate collector with a 20 m² surface area [4]. American engineers H. E. Wilsie and J. Boyle, Jr., installed several solar engines, flat collectors, and tubular heaters within the borders of the United States. They used a mix of water with ammonia, carbon dioxide, sulphur dioxide, etc., as working fluids and the efficiency of the devices ranged between 50 to 85%. Figure (1.4) shows the image of Shuman's flat-plate collector, published in the Engineering News Journal in May 1909, which is a shallow basin covered with glass to convert solar energy into heat energy by working fluids in a storage tank, used to run the engine to pump water to farms in California [5].

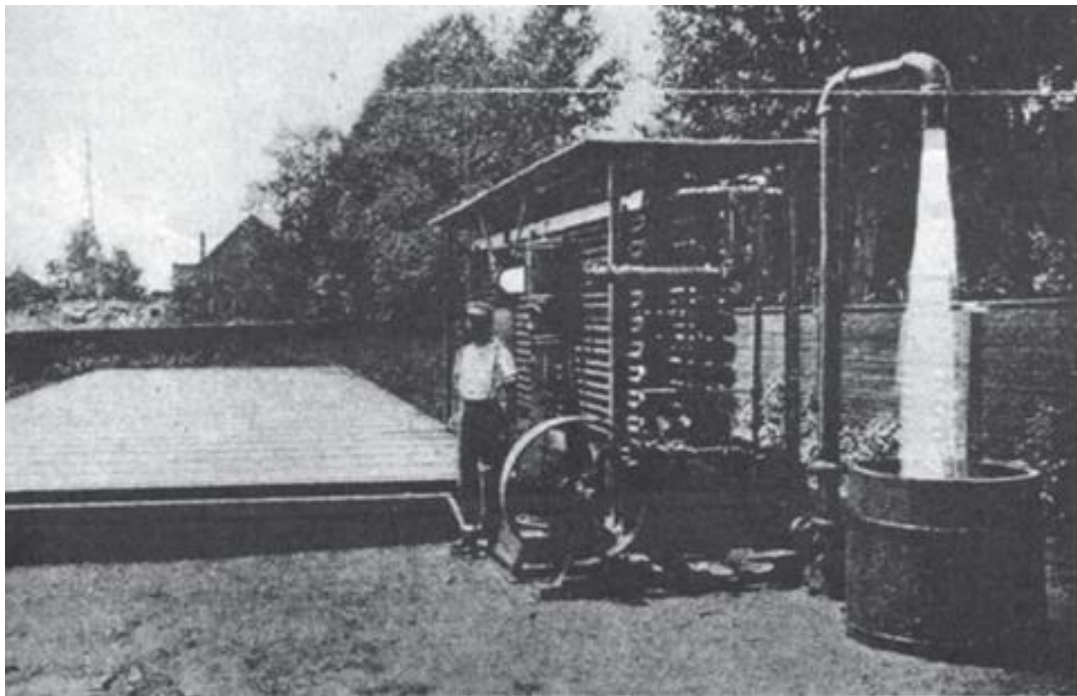


Figure 1.4: Shuman's flat plate collector sun power system

(Adopted from [5])

Hottel and Willis in 1950 developed the first accurate model of flat plate solar collector for water heaters. Thereafter very quickly in many countries of the world, blossomed designs of what is considered a thermo syphon system, flat-plate solar collectors with surface area of 3-4 square meters and a 150-180 liter storage tank [4],[5].

1.1.3 The sun

The Sun is the main source of radiant energy available to the Earth. Our Sun the nearest star to Earth, provides the energy in the form of radiation that travels through space by electromagnetic waves or photon bunches (depending which theory one espouses). The value of the solar irradiance on a surface normal to the sun's rays, also known as the solar constant is estimated to be 1.367 kilowatts per square meter (kW/m^2) at the outer limits of earth's atmosphere. Water vapour, carbon dioxide, and to a lesser extent oxygen, selectively absorb and change the spectrum of the radiation that reaches the ground (and make the sky look blue). For a typical cloudless atmosphere in summer and for zero zenith angle, the 1367 W/m^2 reaching the outer atmosphere is reduced to 1050 W/m^2 direct beam radiation, on a horizontal surface at ground level. The sun produces energy more than humanity's current needs (10,000 times) [6].

Basically, solar energy can be converted and used by the following techniques: Helio-chemical, Helio-electrical and Helio-thermal. The last one (Helio-thermal), is when Solar Energy is converted by solar collectors to heat energy and can be used in several applications, mainly water heating and building heating needs, whether industrial or household [7].

1.2 Problem statement

Due to rising energy prices and growing environmental problems electric heating has become less attractive. By implementing solar water heating for domestic and/or industrial use, a reduction of 70-90% of heating costs and energy consumption can be expected [8]. This research seeks to contribute at improving the efficiency of the solar flat collector, thus possibly reducing the financial burden and the environmental issues.

1.3. Parameters that affect solar flat plate collector

The efficiency of the Collector is affected by several factors, such as location, intensity of solar radiation, wind speed, dust, shade and manufacturer's material properties of the Collector. These parameters can be classified into two parts, climatic and design parameters.

1.3.1 Climatic parameters

- **The intensity of solar radiation**

Solar radiation is the most important of all the natural factors that affect the efficiency of the collector. The intensity of solar radiation is affected by many factors such as location i.e. longitude and latitude, atmospheric condition such as clouds, dust, and the time of the day and season in the year [7],[9], [10].

- **Dust**

Effects of dust and dirt on the cover reduce absorptivity. It is estimated that the percentage loss in solar energy absorptivity in the moderate climates is 1%, and in dry climates it is 2%. The effect of dust depends on the cover type for example, plastic attracts dust or picks up more dust than glass [7],[10].

- **Shading**

Shade also reduces the efficiency of the collector. Particularly it has an effect on large systems for units neighbouring in a row, where shadow depends on the distance between the collectors, the length of the row, the angle of inclination, the time of the day season in the year and latitude [10], [11].

- **Wind**

Wind speed increases result to increasing the amount of heat loss to the ambient and definitely minimizes the efficiency of the collector [12].

1.3.2 Design parameters

- **Plate**

Plate surfaces that have high absorptivity of solar radiation and low emissivity are required. Shukatme [13] claims that the selective absorber plate surfaces were first

suggested by (Tabor, 1956) and (Dunkle, 1958). The plate collector should have the ability to absorb the largest amount of solar radiation, and transfer the heat to a liquid at minimum temperature difference and minimize the heat loss to the surroundings [14],[15].

- **Glazing**

The most important properties of the cover over the solar absorbers plate are reflection (ρ), absorption (α), and transmission (τ). The reflection and absorption of the covering should be as low as possible and the transmission (τ) as high as possible for maximum efficiency. Glass and plastic are the materials used to cover flat plate solar collectors, but the latter does not tolerate sunlight for long. It is recommended to put a cover of glass and plastic and evacuate the air between them to minimize convection loss. Plastic is usually placed under the glass cover to protect it from sunlight and heat; and extend its lifetime of service [14],[15].

- **Tube spacing**

According to Duffie and Beckman [10], it is clear that a small distance between the tubes increases efficiency. In the case of touching the tubes together leads to the dispensing of the plate; however it leads to an increase in the price of the collector. The space between tubes depends on several factors; the most important is the cost of the metal, the plate thickness and the tube diameter. As a result the space between the tubes is different from one region's manufacturer to another [16].

- **Tilt angle**

The orientation of the collector, the azimuth angle and incidence angle has a significant effect on the amount of solar radiation falling on the collector. Generally, the collectors are fixed and do not trace the sun's travel. The best tilt angle of the collector is facing the sun's travel at an angle approximately equal to the site's latitude [17].

1.4. Project objectives

The main objective of this research is to investigate or determine the efficiency of the collector on the basis of geometry per unit area productivity. The work will be directed to a particular manufacturer's design on the proportionality of their units. The geometry of the panels (such as rectangular short or long sides and square) is expected to affect-the

amount of heat acquired because of the number and length of the tubes attached to the absorbent plate, as well as the geometry affecting heat losses due to prevailing atmospheric conditions. It is intended to test specially manufactured flat plate collectors (provided by a local manufacturer) with the proviso that all three geometries will have identical total surface area.

1.5. Significance of the thesis

The importance of this research is in optimising the design geometry of flat plate collectors as a guide to commercial manufacturers. More efficient solar water heating systems would lead to encourage consumers to replace conventional (electrical) water heaters, which will contribute toward energy savings.

1.6. Limitations of the thesis

This research will focus on a comparison of the efficiency between three flat plate collectors that have identical solar energy receiving area and will be conducted in a laboratory where their orientation and tilt angle will be kept constant. Solar irradiation will be provided by an array of controllable flood lights.

1.7. Organization of the thesis

This study is organised as follows:

Chapter One provides the motivation for the current study and general background information on the energy crisis, historical overview on solar energy and general related information about the sun, as well as some parameters that affect solar flat plate collector.

Chapter Two presents the theoretical background of solar energy, heat transfer, and related equations to calculate the solar water heating system's efficiency and acquired energy and dimensional analysis of the variables that affect flat plate solar collectors.

Chapter Three describes the construction of the solar thermo-syphon water heating system, the instrumentation used and the experimental protocol for testing the system.

Chapter Four reports and discusses the results of the experiments and the dimensional analysis performed.

Finally, the main conclusions of the study are summarised in Chapter 5 where a brief attention is also given to recommendations for further investigations.

CHAPTER TWO THEORETICAL BACKGROUND

2.1 Solar energy

Clean energy generated from the sun could be much more than what is needed by humans. Sun sends an amount of solar radiation in one day to generate enough energy for a year. For example: 10% of sunlight is equivalent to 20 TW that is double the global consumption of fossil energy [18].

However there are several reasons that stand as obstacles when humans attempt to benefit from the sunshine available on the earth's surface. The most important reasons: The Earth's rotation around its axis makes solar radiation available at a given location for a shorter period during the day. The atmosphere/cloud covers etc. absorb about 19% and reflect about 26% of the solar radiation. Of the 55% remaining solar radiation that reaches the ground, another 4% is reflected leaving 51% to be absorbed by the earth, or used in photosynthesis, in heating the surface and the lower atmosphere, melt ice and evaporate water see figure (2.1) [19].

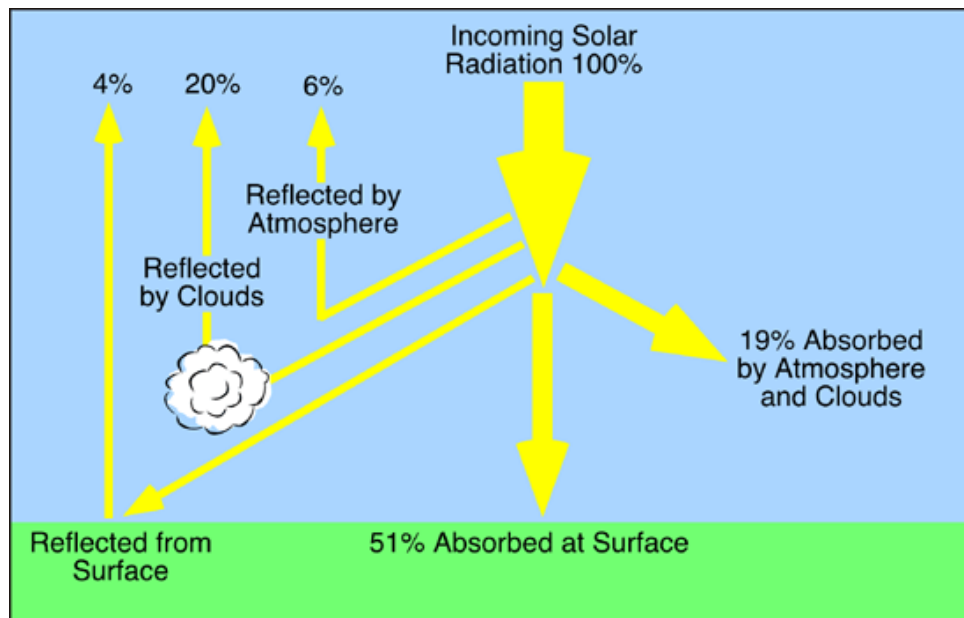


Figure 2.1: Schematic representation of solar radiation on Earth

(Adopted from [20])

Figure (2.2) shows the heat balance on a flat plate solar radiation collector, where the amount of heat absorbed by the plate is about 80% of the incoming radiation of which an amount of 35% is attributed to losses with a remainder of only 45% of the incoming radiation as useful heat [18].

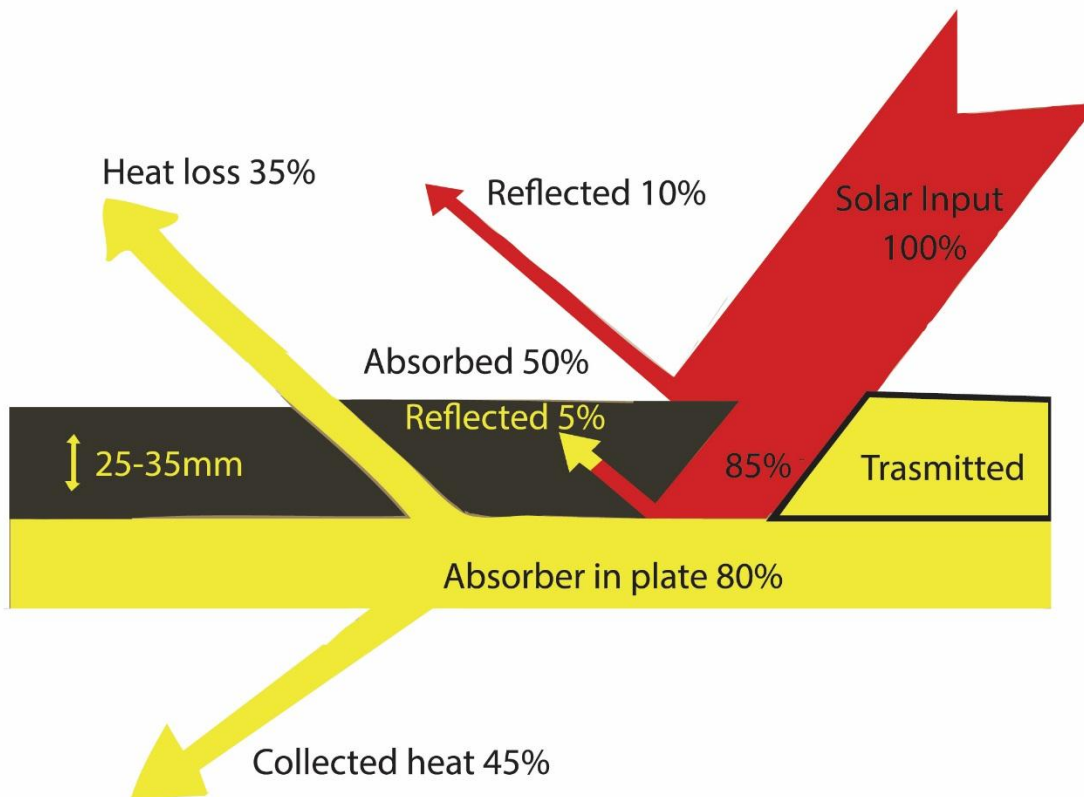


Figure 2.2: Schematic of the heat balance on a flat plate solar radiation collector (Adopted from [21])

The sun's energy is available on the surface of the earth in the form of radiation energy and its absorption and transmission through the various materials (utilized in thermal heating systems) are based on the principles of heat transfer [22].

A solar energy flat plate collector generates useful heat, when part of the sunlight is absorbed by the absorber plate. In steady state conditions, the useful heat generated by

the flat plate solar energy collector must be equal to the total energy arriving at the collector (input) minus the loss to the surroundings. An efficient collector enhances the heat transfer to the absorber plate or fluid flowing through it and reduces the heat loss to the surroundings [10], [13].

2.2 Heat Transfer

Heat transfer is defined as the transmission of thermal energy from one point to another as a result of a temperature difference between them. Understanding the heat transfer mechanisms is very important in various applications of modern technology. Heat is transferred by the fundamental modes/mechanisms of conduction, convection and radiation individually or in any combination of them [7].

2.2.1 Conduction

Conduction is defined as the automatic transfer of thermal energy through direct contact with the particles of an area at high temperature to another area that has a lower temperature [7]. Conduction heat transfer depends on the property of the material known as thermal conductivity (k), the area and thickness or distance (dx) separating the two areas, as well as the difference in temperature (dt) between them. The rate of heat transfer by the conduction mode \dot{Q}_{cond} is expressed via the known "Fourier law of heat conduction" [23], [24].

$$\dot{Q}_{cond} = -kA \frac{dt}{dx} \quad (2.1)$$

Where k is the thermal conductivity of the material (W/mK),

A is the heat transfer area (m^2),

dt/dx is the temperature gradient ($^{\circ}K /m$).

2.2.2 Convection

Convection is the mode of heat transfer that takes place by the mass motion of a fluid in contact with a solid surface either at a relative higher or lower temperature. Moving thermal energy by fluid density changes creating a flow between different layers or regions is called Free or natural Convection. Forced Convection is when the energy is transferred when the motion of the fluid is established by an external force, such as a fan

or pump. In general, the rate of heat transfer by convection between a solid surface and a fluid \dot{Q}_{conv} is given by Newton's law [7], [23].

$$\dot{Q}_{conv} = hA_s(T_s - T_f) \quad (2.2)$$

Where h is the convection heat transfer coefficient in ($W/m^2 \text{ } ^\circ C$),

A_s is the solid's surface area through which convection heat transfer takes place (m^2),

T_s is the surface temperature and T_f is the temperature of the fluid ($^\circ C$).

2.2.3 Radiation

Thermal radiation heat transfer mode is known as the energy emitted by a body at a given temperature by electromagnetic waves ($0.1 \mu m - 100 \mu m$). Radiation heat transfer does not need a medium to propagate [7], [25].

For real surfaces, the radiation emitted \dot{Q}_{emit} is expressed by:

$$\dot{Q}_{emit} = \varepsilon \sigma A_s T_s^4 \quad (2.3)$$

Where ε is the emissivity of the surface, $0 \leq \varepsilon \leq 1$

σ is the Stefan-Blotzmann constant, $\sigma = 5.67 \times 10^{-8} \text{ (kg s}^{-3} \text{ K}^{-4}\text{)}$,

A_s is the surface area of the emitter (m^2),

T_s is the absolute temperature of the surface ($^\circ K$).

2.3 Important equations to calculate the solar water heating system's efficiency and acquired energy.

To simplify the thermal analysis performed on the flat plate solar energy collector the following assumptions were applied:

- The flat plate solar energy collector was thermally in steady state.
- The solar radiation on the flat plate collector plate was uniform.
- Dust and dirt on the collector's surface were negligible.
- Shading on the absorber plate was negligible.
- There was no variation in the ambient temperature during the tests.

Note that, this being a comparative study of the hot water system's efficiency based on a simple geometric solar energy collector's configuration, calculations of heat losses by radiation and convection, for each solar collector were not necessary.

2.3.1 Energy input to the collector

The amount of the input heat on the collector can be calculated if the intensity of solar radiation falling on the surface area of the collector is known [7]:

$$Q_i = I \cdot A \quad (2.4)$$

Where: Q_i is the heat input to the collector (W),

I is intensity of solar radiation W/m^2 ,

A is the collector's surface area exposed to the sun's irradiance $.m^2$.

2.3.2 Energy acquired by the geyser

Through the heat exchange between the plate of the collector and the fluid passing through its pipes, the energy/heat was transferred to the water of the geyser (i.e. the heat was stored in the water of the geyser). The amount of the absorbed or gained heat energy on the geyser's water can be calculated (say hourly) by taking an average of the temperatures of the water at the various positions inside the geyser, during such time intervals [7], [10].

$$Q_o = \frac{m C_p T_{avg}}{\Delta t} \quad (2.5)$$

Where Q_o is the heat acquired by the water in the geyser (W), m is the mass inside the geyser (kg), T_{avg} is the average temperature inside the geyser recorded (i.e. average of six temperatures inside the geyser) ($^{\circ}C$), Δt is the time interval i.e. an hour = 3600 seconds. C_p is the average specific heat of the water (4186) Joules/kg $^{\circ}C$.

2.3.3 Solar water heating system's efficiency

The solar thermo-syphon system's efficiency depends on its ability to absorb the sun's irradiance by the collector and turn it into a useful heat energy stored in the geyser. This is expressed by the following equation [7].

$$\eta = \frac{Q_o}{Q_i} = \frac{mC_p T_{avg} / \Delta t}{I \cdot A} \quad (2.6)$$

Where η is the solar thermo-syphon system efficiency, and all other quantities as described in the equations (2.4), (2.5), respectively.

2.4 Dimensional analysis

Dimensional analysis is a relatively simple mathematical method used to predict the relationship of physical parameters that influence the behaviours of phenomena in the fields of fluid mechanics, thermodynamics, heat transfer, solid mechanics etc. The simplest analysis involves the basic fundamental units of dimensions MLT: mass, length, and time, and all the variables (expressed in these fundamental dimensions) assumed to influence a given phenomenon [26], [27].

2.4.1 Finding a functional relationship between variables by the Buckingham Π Method

The derivation of three dimensionless numbers using the Π Buckingham theorem/method that was performed on the parameters affecting a flat plate solar collector yielded a functional relationship which may be used in enhancing solar water heating systems' design [28]. The parameters affecting the phenomenon of a solar energy collector were assumed to be:

Δp is the pressure difference between inlet and outlet of the flat plate solar energy collector ($\text{kg}/\text{m} \cdot \text{s}^2$),

ρ is the density of the water flowing through the collector (kg/m^3),

g is earth's gravity (m/s^2),

I is the amount of solar radiation incident on the collector's surface. ($\text{W}/\text{m}^2 = \text{kg} \cdot \text{m}^2/\text{s}^3$),

h is the water's specific enthalpy (flowing through the collector) ($\text{Joules}/\text{kg} = \text{m}^2/\text{s}^2$),

L is the vertical height difference between input cold water and output hot water of the collector as inclined facing the sun (m).

Using the Buckingham Π Theorem with the parameters:

Δp , ρ , g , L , I , h and the basic fundamental dimensions of mass, length and time.

The Buckingham theorem predicts the number of Π numbers from [26], [29]:

Where m (fundamental dimensions) = 3, n (the physical variables involved) = 6, thus there will be $n - m = 3$ Π groups as shown:

For the Π_1 group involving the variables L g ρ Δp

$$(M^0 L^0 T^0) = L^a (L T^{-2})^b (M L^{-3})^c (M L^{-1} T^{-2})$$

Expanding and collecting like units, the exponents can be solved as:

$$\text{For M: } 0 = c + 1 \Rightarrow c = -1$$

$$\text{For L: } 0 = a + b - 3c - 1 \Rightarrow a + b = -2$$

$$\text{For T: } 0 = -2b - 2 \Rightarrow b = -1 \text{ so } a = -1$$

This means that, Π_1 , is

$$\Pi_1 = L^{-1} \rho^{-1} g^{-1} \Delta p = \Delta p / (L \rho g) = \frac{\Delta p}{L \rho g} \quad (2.7)$$

For the Π_2 group involving the variables L g ρ I ,

$$(M^0 L^0 T^0) = (M L^{-3})^a (L T^{-2})^b L^c (M L^{-1} T^{-3})$$

Solving for the exponents,

$$\text{For M: } 0 = a + 1 \Rightarrow a = -1$$

$$\text{For L: } 0 = -3a + b + c - 1 \Rightarrow a + b = -2$$

$$\text{For T: } 0 = -2b - 3 \Rightarrow b = -1.5 \text{ so } a = -0.5$$

Thus the second dimensionless Π_2 is

$$\Pi_2 = \rho L^{-1/2} g^{-3/2} I = I / (\rho L^{1/2} g^{3/2}) = \frac{I}{\rho L^{1/2} g^{3/2}} \quad (2.8)$$

For the Π_3 group,

$$(M^0 L^0 T^0) = (M L^{-3})^a (LT^{-2})^b L^c (L^2 T^{-2})$$

Solving for the exponents,

$$\text{For M: } 0 = a + 0 \Rightarrow a = 0$$

$$\text{For L: } 0 = -3a + b + c + 2 \Rightarrow b + c = -2$$

$$\text{For T: } 0 = -2b - 2 \Rightarrow b = -1 \text{ so } c = -1$$

Thus the third dimensionless Π_3 is

$$\Pi_3 = L^{-1} g^{-1} h = h / (Lg) = \frac{h}{Lg} \quad (2.9)$$

Thus, the three Π groups can be written together as

$$f(\Pi_1, \Pi_2, \Pi_3) = \left(\frac{\Delta p}{L \rho g}, \frac{I}{\rho L^{1/2} g^{3/2}}, \frac{h}{Lg} \right) = 0$$

Finally rearranging one can indicate a possible relationship between them.

$$\frac{\Delta p}{L \rho g} = f\left(\frac{I}{\rho L^{1/2} g^{3/2}}, \frac{h}{Lg}\right) \quad (2.10)$$

2.4.2 Finding or calculating the difference in pressure between the inlet and outlet of the flat plate solar energy collector

The pressure difference between the inlet (point A) and outlet (point B) of the collector as shown in the figure (2.3) was calculated based on the vertical height of water and the density depended on the temperature of the water (i.e. cold or hot) through the system.

$$P_A = P_0 + [\rho_{avg} x_1 + \rho_{cold} x_2]g$$

$$P_B = P_0 + [\rho_{hot} x_1 + \rho_{hot} x_3]g$$

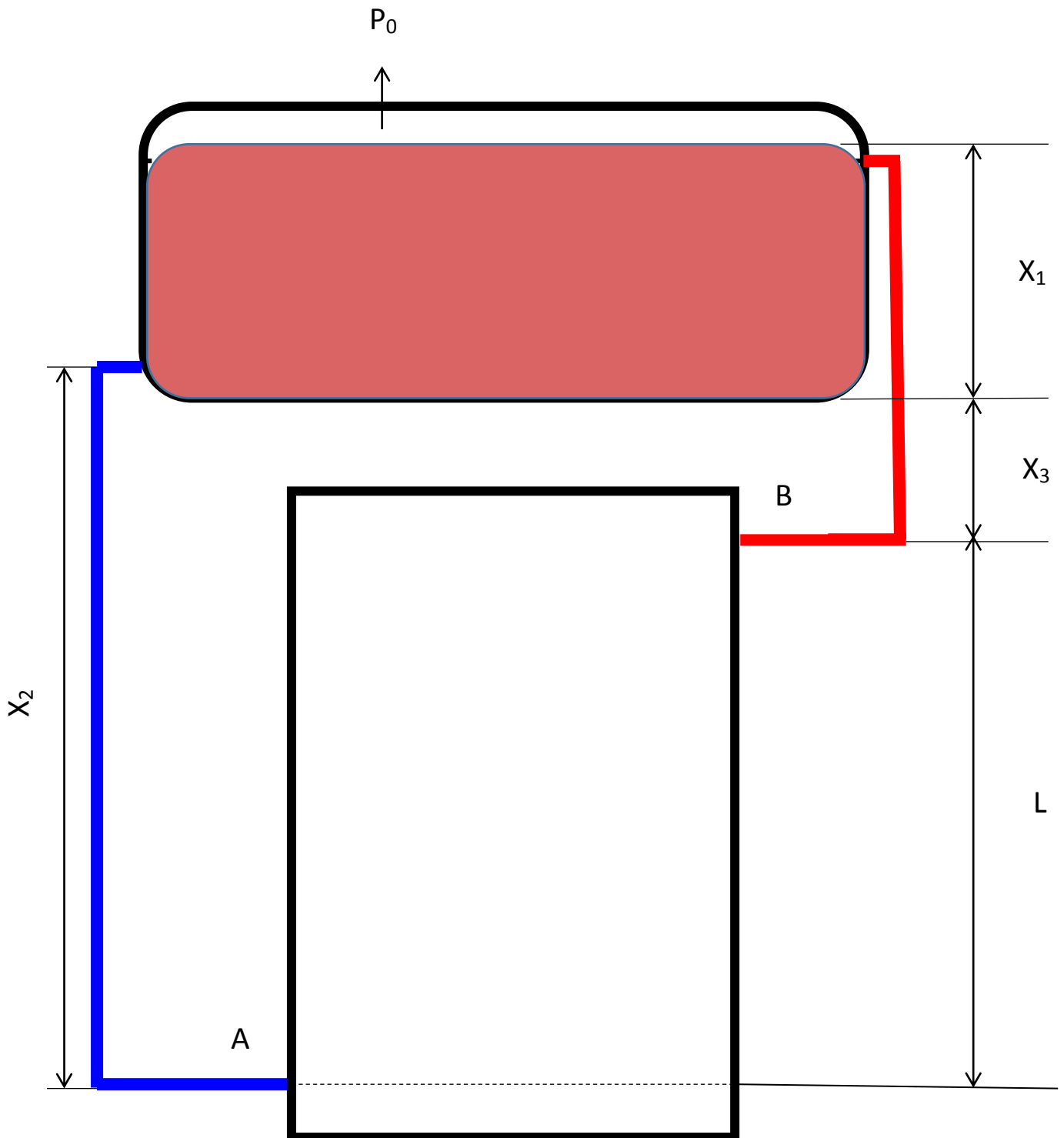


Figure 2.3: Schematic diagram of the calculation of the static pressure difference across inlet and outlet of the flat plate solar energy collector.

The pressure value at point A and B is influenced by the atmospheric pressure because the system is open to the ambient; hence the difference in pressure between inlet and outlet of the collector (point A and B) is as follows:

$$P_A - P_B = [\rho_{avg} x_1 + \rho_{cold} x_2]g - [\rho_{hot} x_1 + \rho_{hot} x_3]g \quad (2.11)$$

Where P_A is the Pressure at the point A,

P_B is the Pressure at the point B,

ρ_{avg} is the density at the average temperature in the geyser,

ρ_{cold} is the density at the temperature in point A,

ρ_{hot} is the density at the temperature in point B,

g is earth's gravity (m/s^2),

x_1, x_2, x_3 are vertical dimensions in figure 2.3 (m).

Equation (2.11) can be rewritten as:

$$(P_A - P_B)/g = \rho_{avg} x_1 + \rho_{cold} x_2 - \rho_{hot} x_1 - \rho_{hot} x_3 \quad (2.12)$$

Further simplification by assuming all the densities are the same or close to the same value, (because the changes of water density are negligible or small), the equation above can be rewritten as:

$$(P_A - P_B)/\rho g = x_1 + x_2 - x_1 - x_3 = x_2 - x_3 = L \quad (2.13)$$

It is noted that equation (2.7) $\Pi_1 = \frac{\Delta p}{L \rho g}$ is identical to the result above.

CHAPTER THREE

THE METHODOLOGY OF THE EXPERIMENTS

This chapter describes the construction of the solar thermo-syphon water heating system, using three flat plate solar collectors with identical 1.5 m² surface area with different collectors' geometrical configurations. This chapter also covers the experimental protocol that was followed in order to compare the effect of the geometrical configuration of the flat plate collector on the efficiency of the thermo-syphon system.

3.1 Description of the thermo-syphon system

A thermo-syphon solar water heating system was installed inside a laboratory in the department of Mechanical Engineering at the Cape Peninsula University of Technology, Bellville Campus, Cape Town, South Africa. The aim was to compare the individual efficiency of the system with each one of three flat plate collectors that have the same surface area but different geometric configuration. The system as illustrated in the schematic diagram figure (3.1) consisted of a geyser and flat plate collector connected through pipes and installed on a frame. A sun simulator was constructed and placed above the flat plate collector as depicted in figure (3.2).

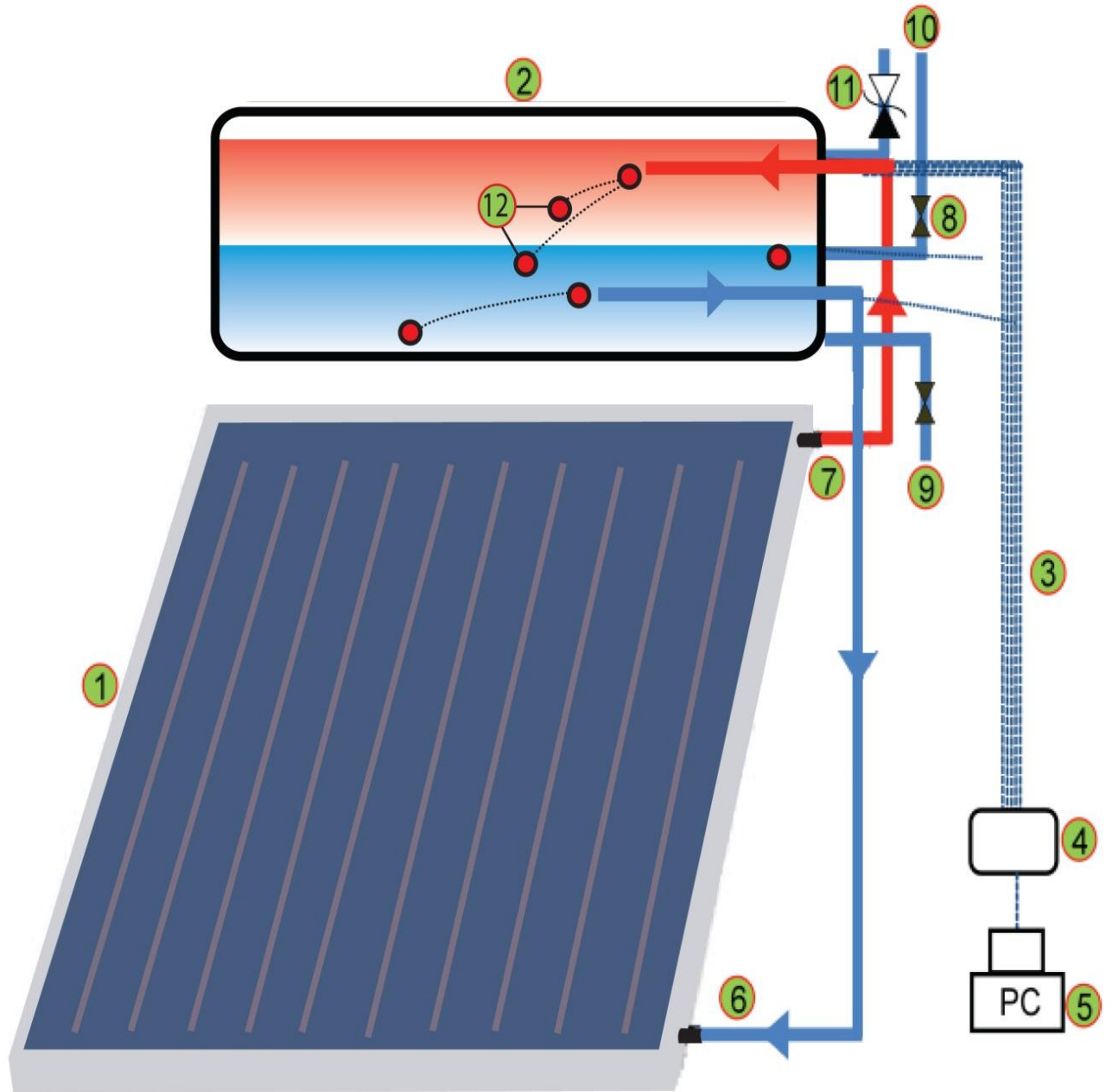


Figure 3.1: Schematic diagram of the thermosyphon system

- | | |
|------------------------------|---|
| 1. Flat plate collector | 2. Geyser/ Tank |
| 3. Thermocouples | 4. Testo 926 digital thermometer |
| 5. Computer | 6. Inlet to the collector |
| 7. Outlet from the collector | 8. Water supply valve |
| 9. Drain valve | 10. Water supply |
| 11. Safety valve | 12. Position of thermocouples in the geyser |

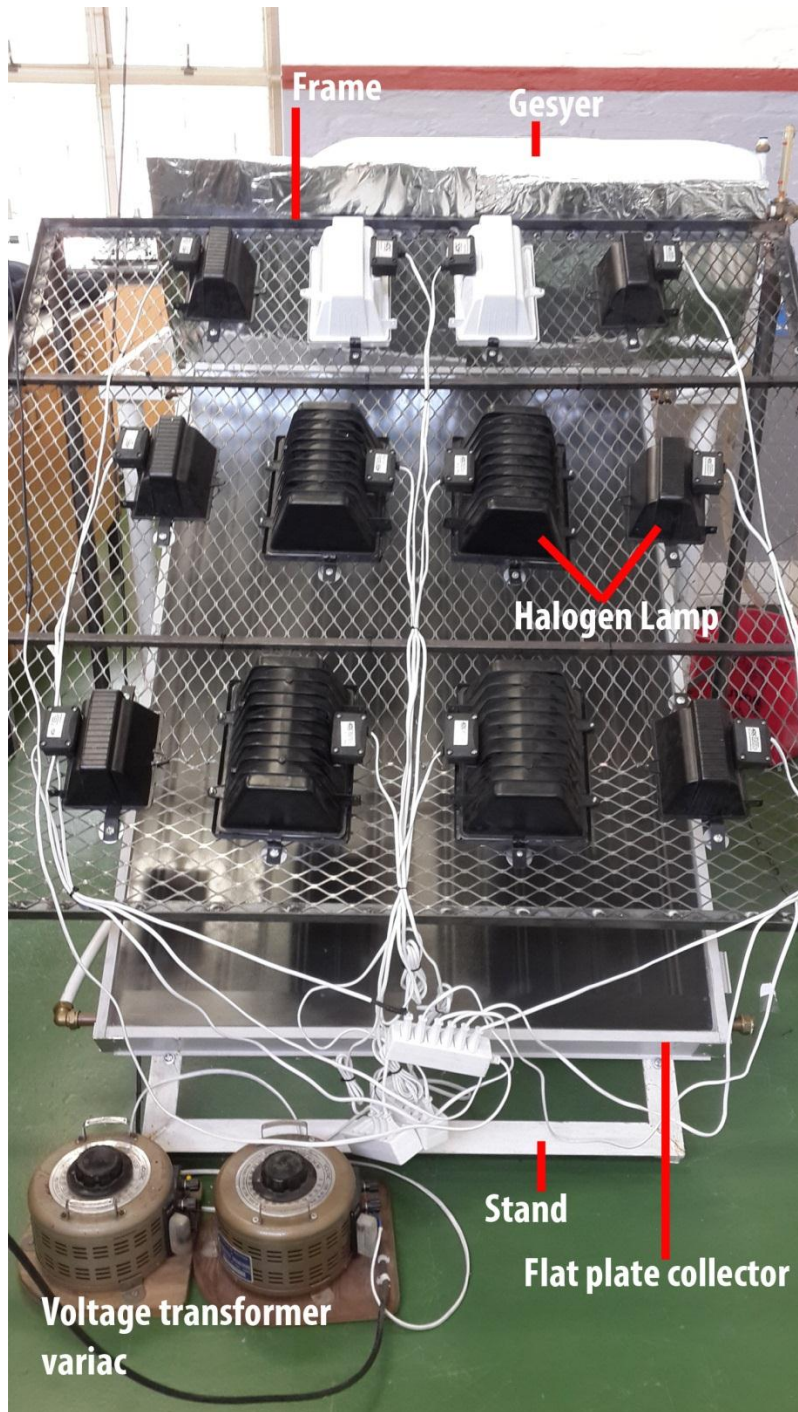


Figure 3.2a: The sun simulator positioned above the solar collector



Figure 3.2b: The geyser's various connections

3.1.1 Geyser

The geyser with a capacity of 100 litres was made of (Epoxy Vinyl Ester and Glass) materials. These materials besides minimizing heat loss to the ambient, are also anti-corrosive, lightweight and stronger than metal on a weight to weight basis. Table (3.1) shows the specifications and dimensions of the geyser. The geyser was installed in a horizontal position [30]. Figure (3.3) shows some details of the geyser's construction.

Table 3.1: The specifications of the geyser
(Adopted from [30])

Capacity	Height	Width	Length	Weight	Working pressure
100 L	480 mm	460 mm	1147 mm	19 Kg	400Kp

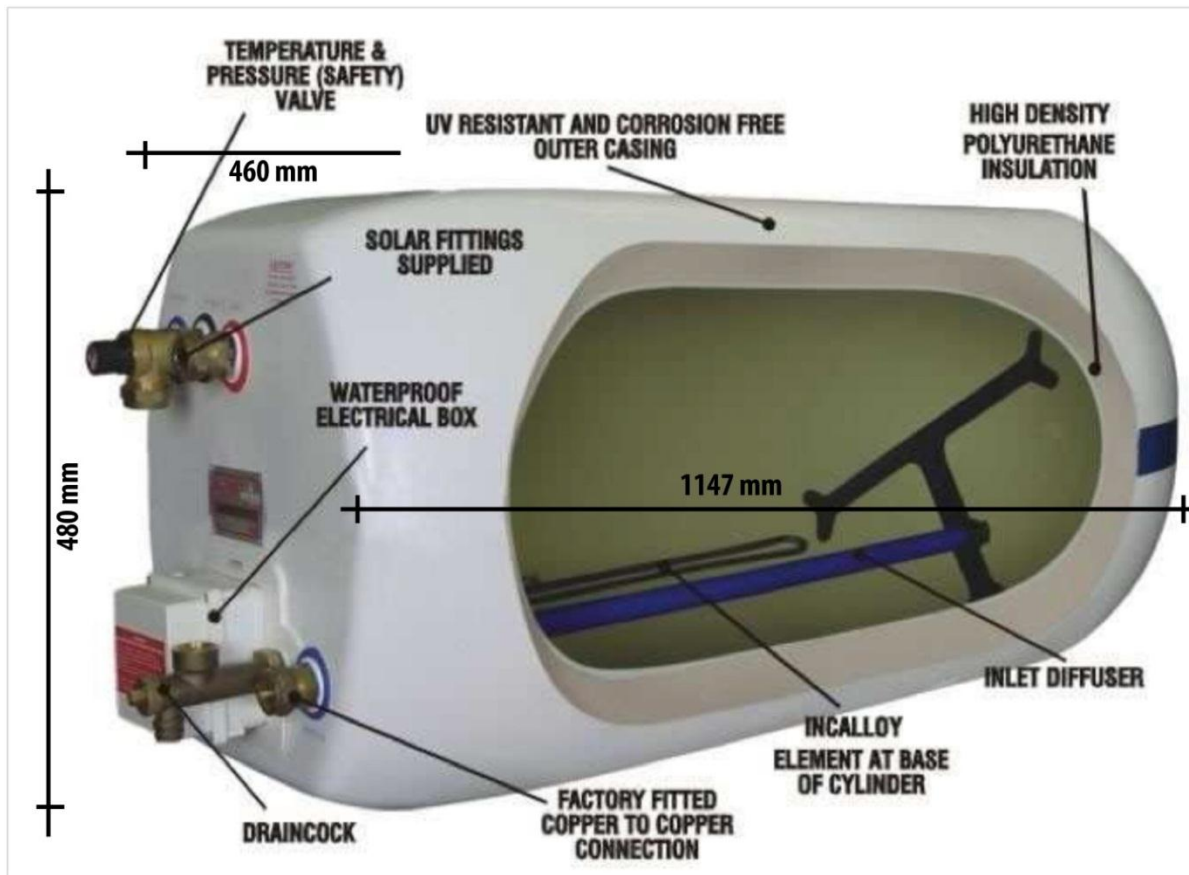


Figure 3.3: Xstream Solar Hot Water geyser
(Adopted from [30])

3.1.2 Flat plate collectors

Three flat plate solar collectors were used (each one individually) with the geyser, in the indoor experiments. All three solar collectors had identical surface area (1.5 m^2) and materials' specifications, however different geometrical configurations. The three flat plate solar collectors were manufactured by SolarMax Company in Kleinmond, Western Cape. Table (3.2) contains the technical specifications and dimensions of the three solar collectors, while figure (3.4) illustrates the differences in their linear dimensions for their particular configuration.

Table 3.2: The specifications of the flat plate solar collectors

(Adopted from [31])

Specifications	Panel A (Vertical)	Panel B (Square)	Panel C (Horizontal)
Area	1.5 m^2	1.5 m^2	1.5 m^2
Dimensions	1500 x 1000 x 75 mm	1230 x 1230 x 75 mm	1000x1500x 75 mm
Risers	8	10	12
Tub spacing	120mm		
Glazing	4mm Toughened One-Way Prismatic Glass		
Absorber Fins	130mm x0.5mm Roll formed Aluminium		
Piping Grid	22mm Copper Header T-drilled to 15mm copper Risers, Brazed with silver/copper		
Insulation	15 mm Polystyrene and 25 mm rock wool		
Casing	1.5mm Extruded Anodized aluminium		
Backing plate	0.5mm Natural aluminium sheeting		

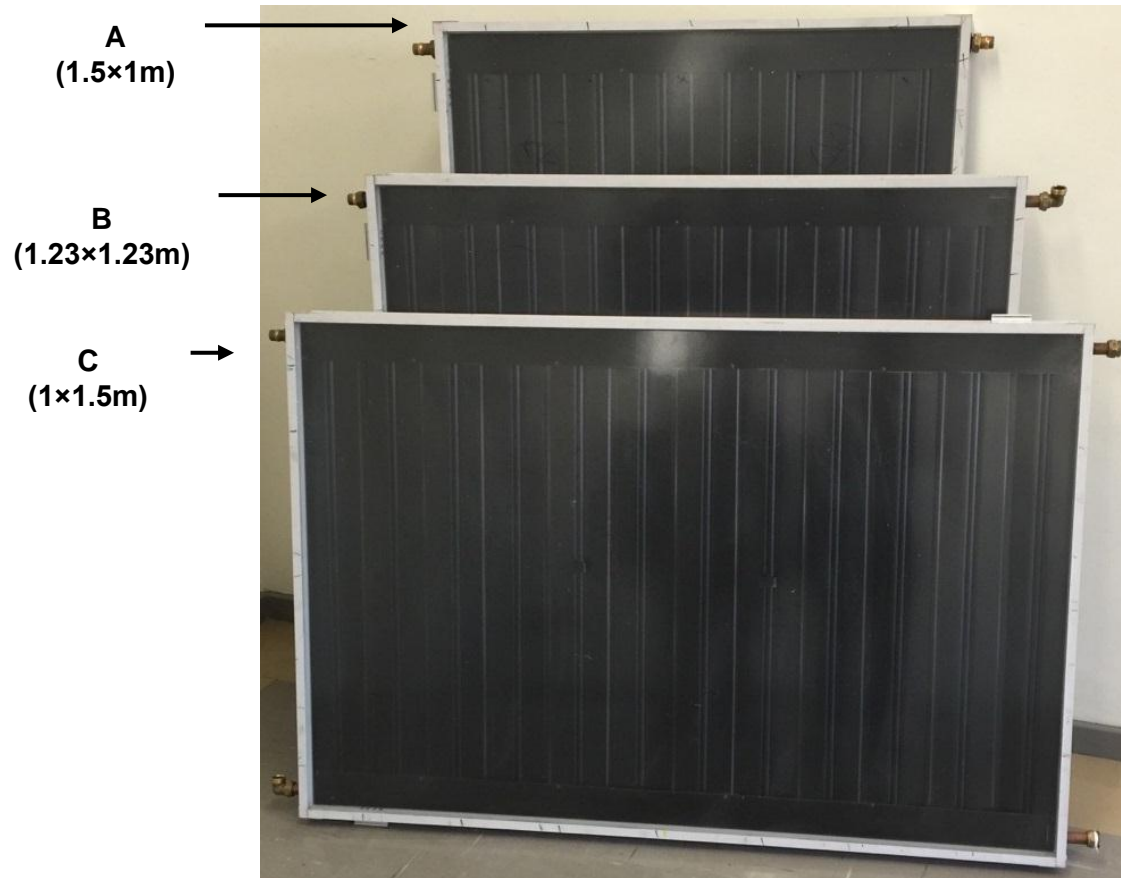


Figure 3.4: The three flat plate collectors

3.1.3 The sun simulator

The Sunlight simulator which was designed to cover an area of 1.5 square meters, consisted of a square frame 1.5 meters made from (30mm×30mm×3mm) angle iron. A wire mesh covered the surface of the frame and acted as support for the twelve halogen floodlights of 1000 W each nominal output power. The spot lights could be appropriately distributed and secured on the wire mesh of the angle iron frame in order to accommodate the shape or geometry of the particular solar collector under test as shown in figure (3.5). They were divided into three groups, and connected to the power supply through variable voltage transformers (Variacs model: SB-10) which enabled control or adjustment of the floodlights' power output. (See Appendix (A-1) for specifications of Variacs).

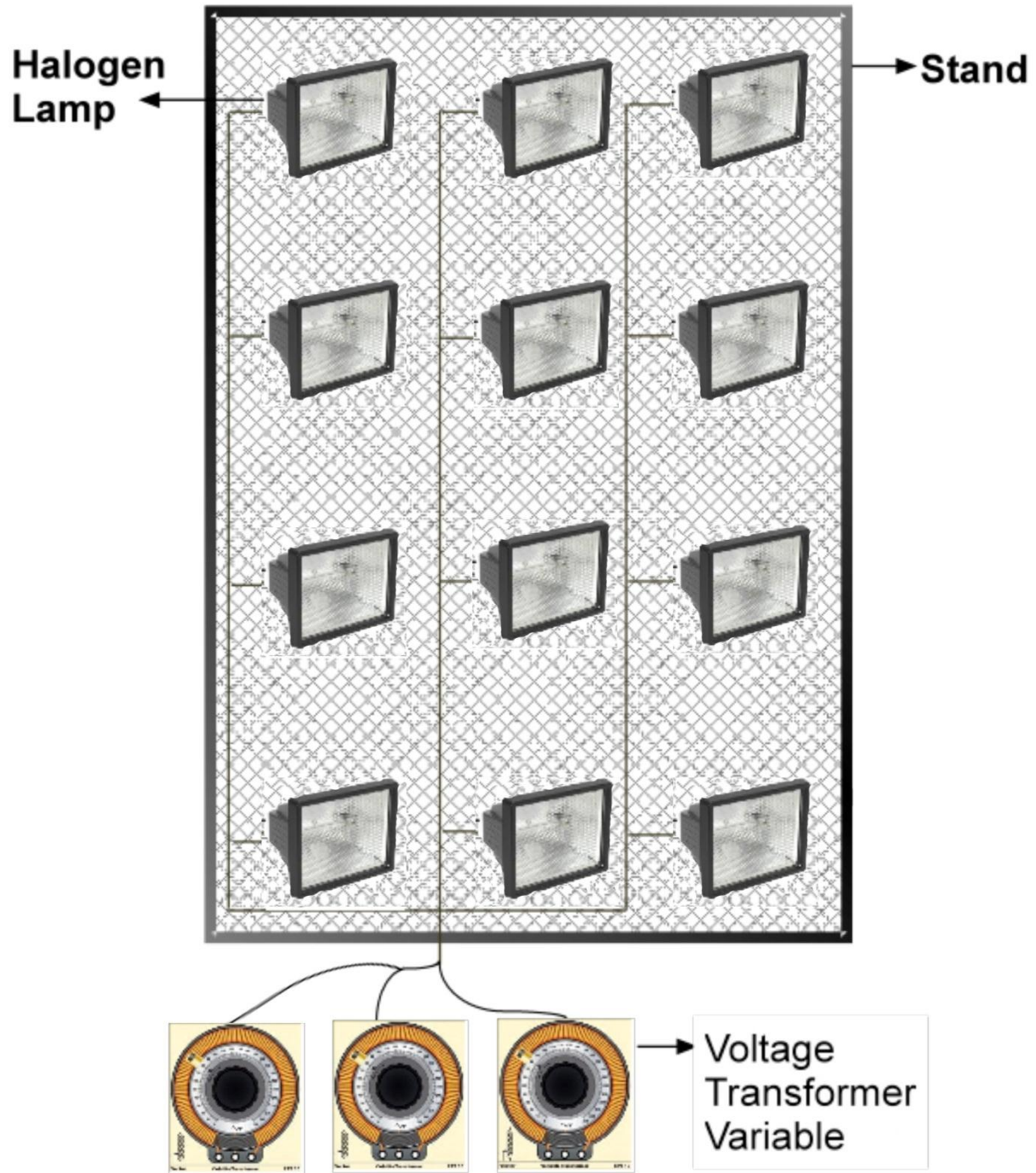


Figure 3.5: The sun simulator

3.1.4 Equipment holder or stand

A steel table was modified to hold the geyser on the top and the solar collector inclined beneath it as shown in figure (3.6). The inclined (35 degrees to the horizontal) part of the stand was long enough to accommodate all three solar collectors. The geyser was secured horizontal at the top of the table and the collectors placed on the inclined part of the stand so that their hot water outlet was in the same place relative to the geyser. For each solar collector the position of their cold water inlet relative to the geyser depended on their length.



Figure 3.6: Equipment holder or stand

3.1.5 Pipe connections

A composite flexible pipe (outer diameter 22mm with thickness 2.5mm) was used in the connections between the solar collectors and the geyser. The composite pipe consists of an aluminium core with inner and outer plastic layers, tightly bonded with a special

adhesive to the aluminium core. The thermal conductivity is 0.45W/m. K, so it saved on insulation material costs [32].

3.2 Instrumentation and experimental protocol

3.2.1 Laboratory's condition

The following steps describe the location and the conditions in the laboratory where the experiment was conducted:

- The experiments were done inside the laboratory in the department of Mechanical Engineering at Cape Peninsula University of Technology Bellville campus, located on Latitude and Longitude: 33.93°S and 18.42°E, respectively.
- Average ambient temperature inside the lab was $20^{\circ}\text{C} \pm 1^{\circ}\text{C}$ during the tests.
- There were no effects of dust and dirt on the surface of the flat plate solar collectors.
- Shadow effects on the surface of the collectors were negligible.

3.2.2 Sun Simulator's radiation intensity measurement

During the experiments, the sun simulator was set to provide an average irradiance of 850 watts per square meter. This value was determined by measuring the intensity of the simulator's radiation on the surface of each flat plate collector (at the beginning of each test) by taking the average of 35 readings using a solar power meter (TES-1333) which is shown in figure (3.7). (See Appendix (A 2) for specifications of the solar power meter).



Figure 3.7: Solar Power meter (TES-1333)

3.2.3 Temperature measurements

The temperatures in the geyser were measured at different levels by inserted T-type (Copper/Constantan) thermocouples which were connected individually via their electrical plugs to the Testo 926 digital thermometer as shown in the figure (3.8). (See appendix (A 3 and A 4) for technical specifications of T-type thermocouple and the Testo 926 digital thermometer, respectively) [34], [35].



Figure 3.8: Testo 926 device and T-type thermocouples

(Adopted from [34], [35])

3.2.4 Experimental Protocol

The closed loop solar thermo-syphon water heating system as is shown in the schematic figure (3.1) was used during experiments that were conducted indoors in order to facilitate collecting the necessary data.

The main reason of conducting the experiments indoors (that is, inside the laboratory) was to avoid environmental variability and thus facilitate further the comparison of the flat plate solar collectors' performance. In this manner the experiments were conducted under the same conditions and with constant power of "solar irradiance" and period of exposure.

Following some preliminary testing which ensured that the instrumentation was performing adequately and that there were no leaks in the system, two day tests were performed for each flat plate solar collector.

The experiments began at 9:00 o'clock and lasted for seven hours with the collector exposed to the sun simulator's irradiance. After a period of "nightly" inactivity of 17 hours where partial cooling of the water in the geyser had occurred, the water was heated again to reach a base line temperature of 53.6 °C (for all three collectors) prior to resuming in the second day the experiment for another seven hours.

The following are detailed steps taken during each experiment.

- Filling the geyser or water storage tank with cold water in the beginning of every test.
- There was no withdrawal of water from the geyser during the experiment.
- Measuring the temperature of water in the geyser with the six type (T) thermocouples every hour \pm 3 minutes.
- Measuring the intensity of solar radiation falling on the plate at the beginning and end of daily irradiation.
- Calculate the average solar radiation.
- Calculate the average temperature of the water in the geyser every hour.
- Calculate the amount of input heat on the plate and the amount of heat acquired in the geyser every hour.
- Calculate the efficiency of the system hourly and the overall (daily) efficiency.

CHAPTER FOUR

RESULTS AND DISCUSSION

4.1 Introduction

This chapter reports on the results of the experimental work that was performed in order to compare the performance of the solar water heating system when using three different (individually of course) of equal surface/collector area flat plate collectors, but of different geometrical configuration. It also presents the results of the dimension analysis that was performed by the author, in order to get a better understanding of the influence of the various parameters that may affect the performance of a flat plate solar collector, while operating with the water being circulated by the conditions of a self-induced thermo-syphon. The experiments were conducted on the water heating system separately with each of the three flat plate solar energy collectors labelled as: vertically long side (A), square (B) and horizontally long side (C). See figure (3.4).

4.2. The test results for the water temperature inside the geyser

The data were processed and calculations were made during the first day and the second day of the experiments, as follows:

- **First day**

The variation of the temperature of the water at different locations inside the geyser during the first day of the test period for collector A is shown in figure (4.1) as a typical example, and in table (B-1) in appendix (B). The water temperature in the geyser starts to increase as expected from 16.4°C to a maximum of 85°C at the surface of the water inside the geyser (T_1) after seven hours, while the minimum temperature of the water (at the lowest position within the geyser) after the same time is increased to 35°C (T_6), obviously due to stratification. See the table in appendix (B-1).

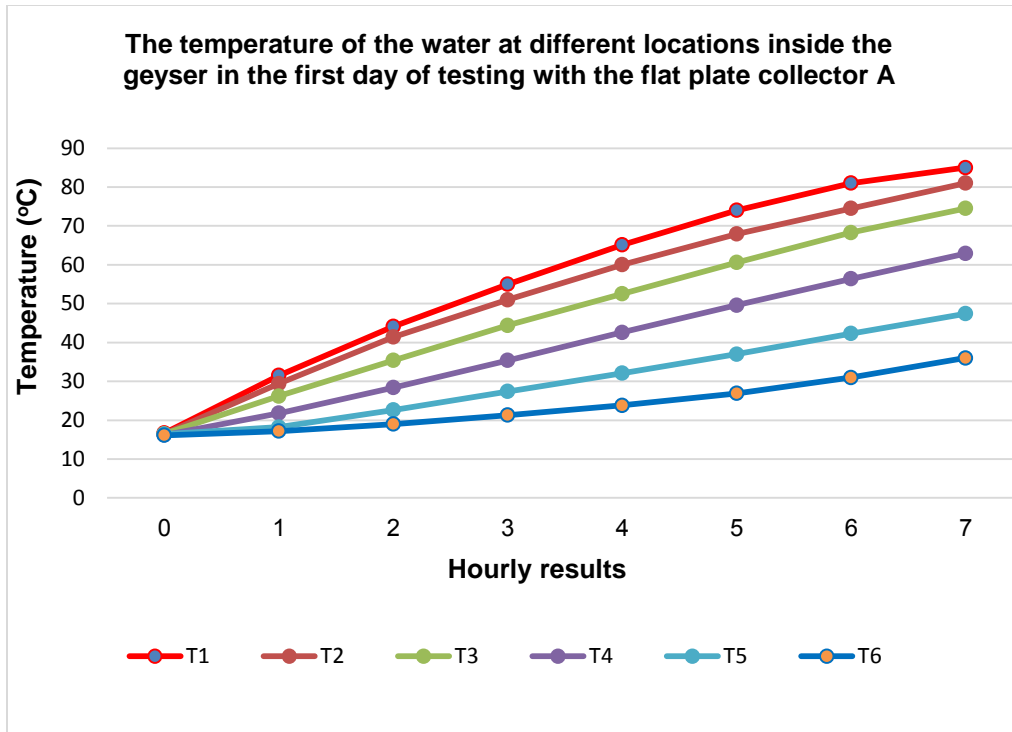


Figure 4.1: Temperature variation of the water inside the geyser in the first day of the test for flat plate collector A

There was a slight difference between the average temperatures of the water in the geyser, toward the end of the first day's testing period, for the three flat plate collectors (A, B, and C) as shown in figure (4.2) and the table (B-1) in appendix (B).

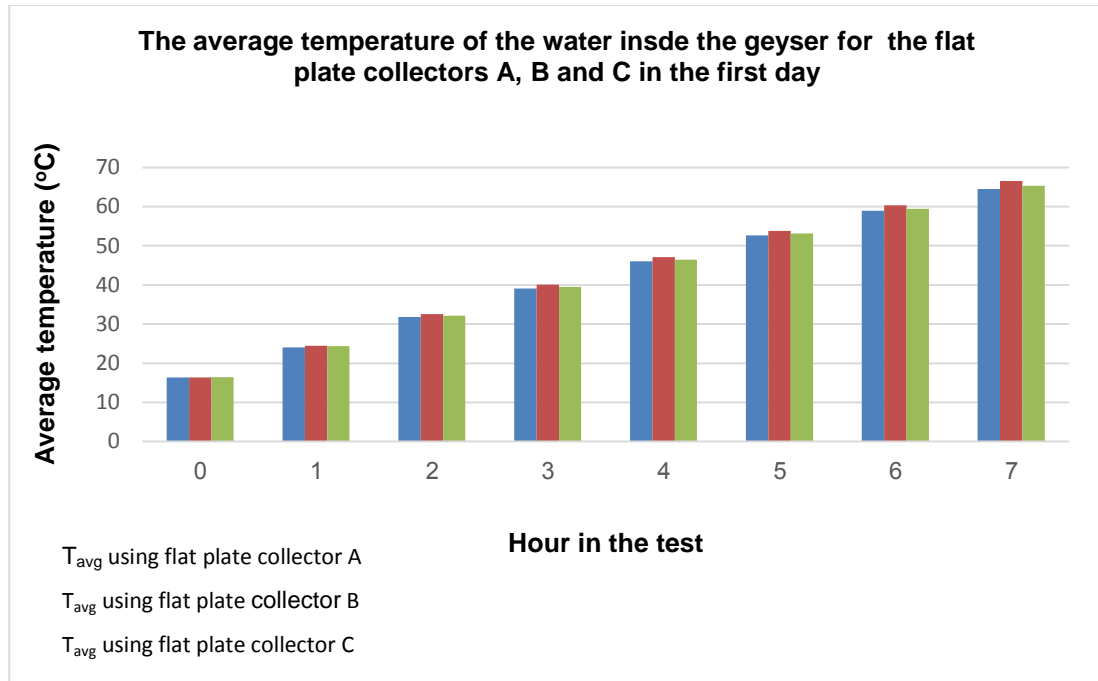


Figure 4.2: Comparison between average temperatures of the water in the geyser when using the flat plate collectors, A, B, and C (first day)

The temperatures of the water in the geyser, for the first two hours, are almost equal when using any of the three collectors, the geyser's water temperature when using collector B begins to show a slight increase (relative to when using collectors, A and C) at the fourth, fifth, and sixth hours. Through to the seventh hour the water in the geyser reached an average temperature of 66.5°C when using collector B, while for collectors A and C it reached 64.5°C and 65.3°C, respectively.

- **Second day**

As a result of cooling i.e. heat lost from the geyser during the night and stratification of the water layers within the geyser, the temperatures recorded at the beginning of the second day of the test using collector A were in the range of 61.1°C and 41.8°C as shown in figure (4.3) and table (B-2) in appendix (B).

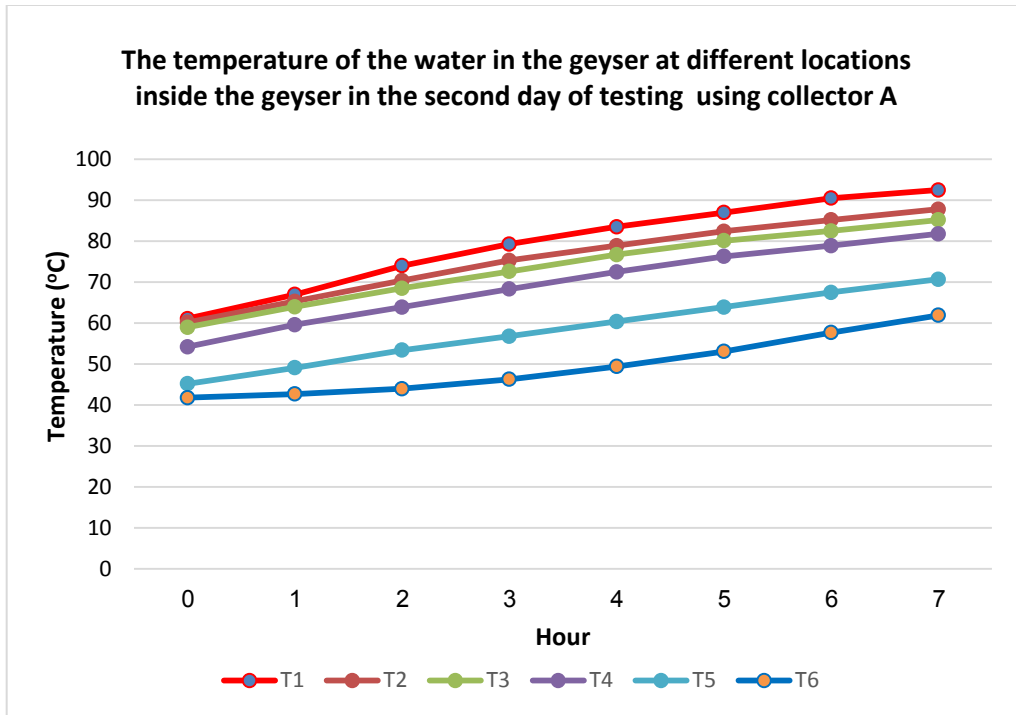


Figure 4.3: The temperature variation of the water inside the geyser during the second day of the test when using collector A

The average temperature of the water in the geyser when using collectors, A, B, and C for the second day is shown in figure (4.4) and the table (B-2) in appendix (B). The average temperatures of the water in the geyser exhibit similar trend to that observed in figure (4.2), that is they are close together in the first four hours, however the highest average temperature of the water in the geyser at the end of the test, was achieved using collector B reaching 86.5°C compared to those obtained using collectors A and C reaching 80°C and 83.2°C, respectively.

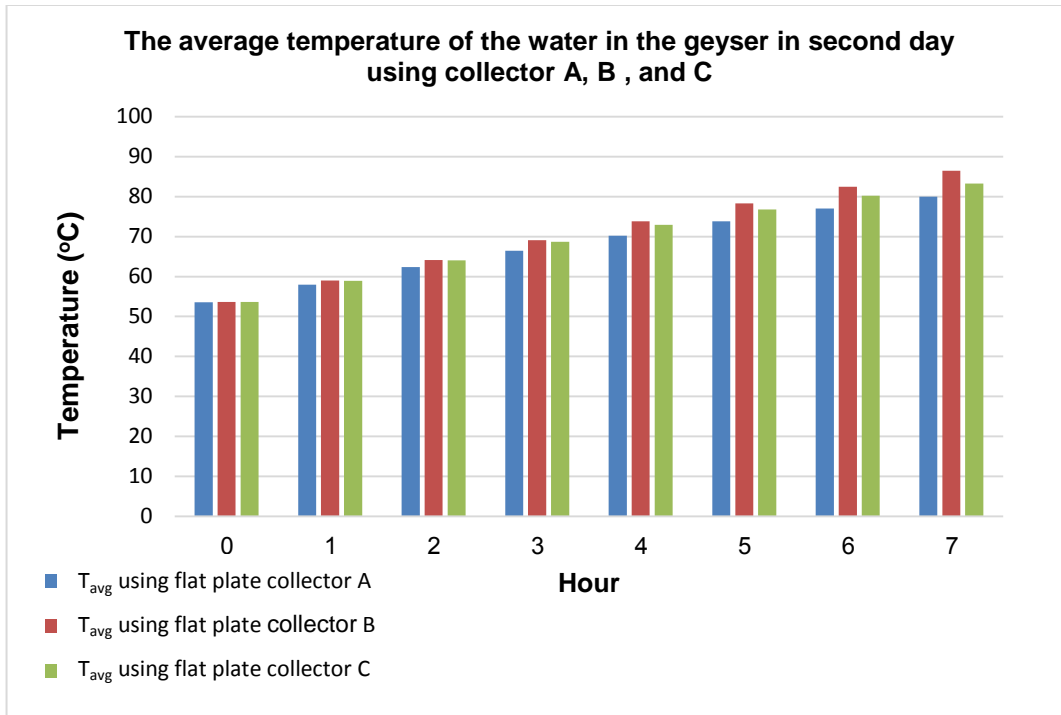


Figure 4.4: Comparison between average temperature of the water in the geyser when using collectors A, B, and C in the second day

4.3 Energy acquired by the water in the geyser

The flow of energy was calculated during the first day and the second day, as follows:

- **First day**

The temperature of the water in the geyser rises continuously through the mixing of the hot water arriving from the collector with the geyser's main mass of water. When the hot water arrives at the top of the geyser it replaces the relatively colder water that leaves the bottom of the geyser to enter the collector. Driven by the naturally induced thermo-syphon this is a continuous process which for all practical purposes can only be dealt with averages within a specified period of time. The average temperature of the water in the geyser was calculated based on the recorded water's temperature, at six different levels in the geyser, on an hourly basis. The energy acquired by the total mass of water (equivalent to 88 litres) in the geyser is simply the product of specific heat of the water and the change of its average temperature during a specific time period (in this case one hour). Figure (4.5) shows that the performance of the collectors in absorbing energy from

what is available in terms of the irradiance from the solar simulator, is better at the early stages of the test because there is a larger temperature difference between the water and the temperature of the absorbers' plates. Total heat delivered by the collectors A, B and C to the geyser was calculated for the first day to be 17.49 MJ, 18.24 MJ and 17.79 MJ, respectively as shown in figure (4.6) where is noted again that collector B performed best. See appendix (D-1) for the calculation of energy rate acquired by the geyser's water (W) and energy accumulated by the geyser's water (MJ) using the collectors A, B, and C.

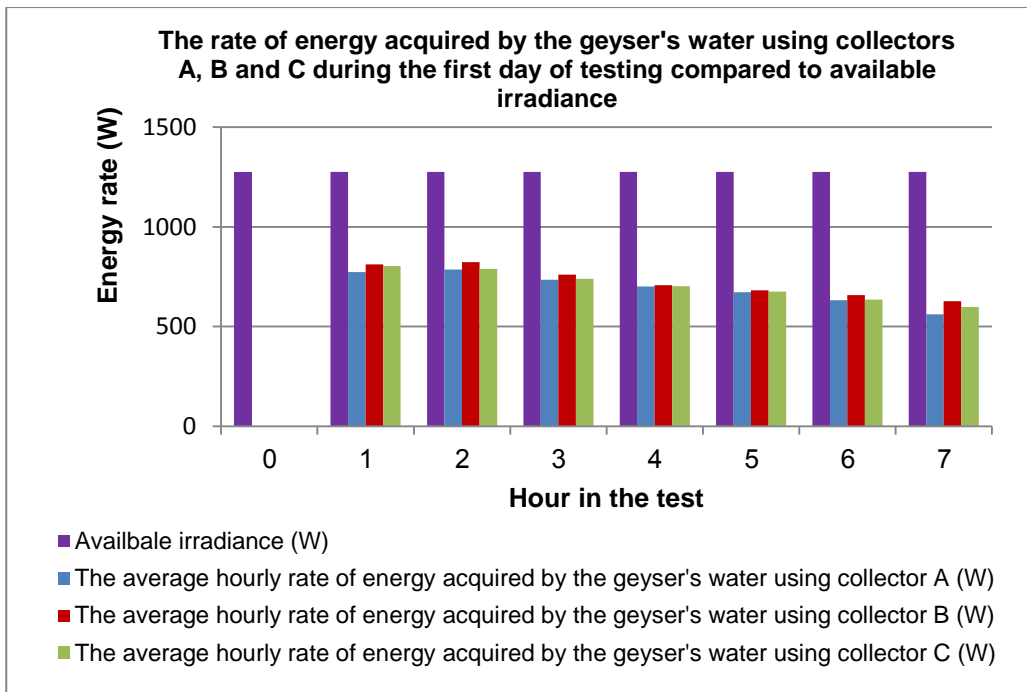


Figure 4.5: Comparison between the rates of energy acquired by the geyser's water using collectors A, B, and C relative to available irradiance during the first day of testing

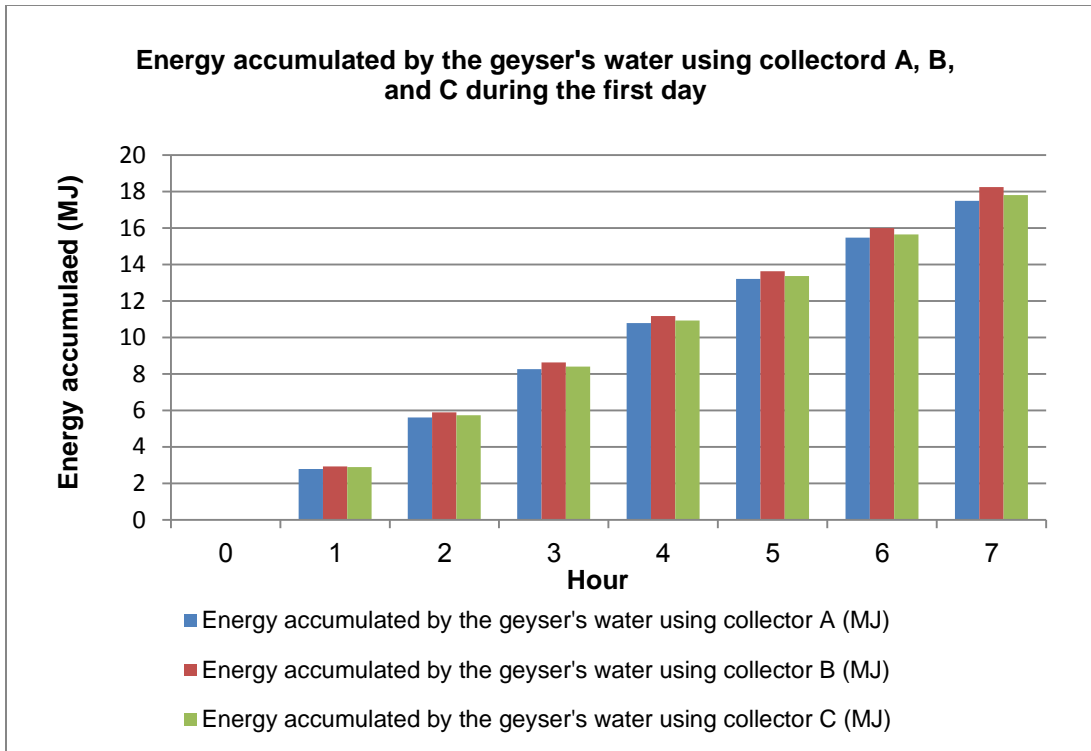


Figure 4.6: Comparison of cumulative energy delivered to the geyser from the flat plate solar collectors A, B, and C during the first day

- **Second day**

As a result of smaller temperature differences between the temperature achieved by the collectors' plates and the water supplied to them by the geyser, their performance decreased on the second day. Figure (4.7) shows the performance of the collectors in absorbing energy from what is available in terms of the irradiance from the solar simulator. However, collector B still performed better as seen from the calculated amounts of energy delivered to the geyser (collectors A, B and C: 23.15 MJ, 25.49 MJ and 24.3 MJ), respectively, as shown in Figure (4.8). See appendix (D-2) for the calculation of energy rate acquired by the geyser's water (W) and energy accumulated by the geyser's water (MJ) using the collectors A, B, and C.

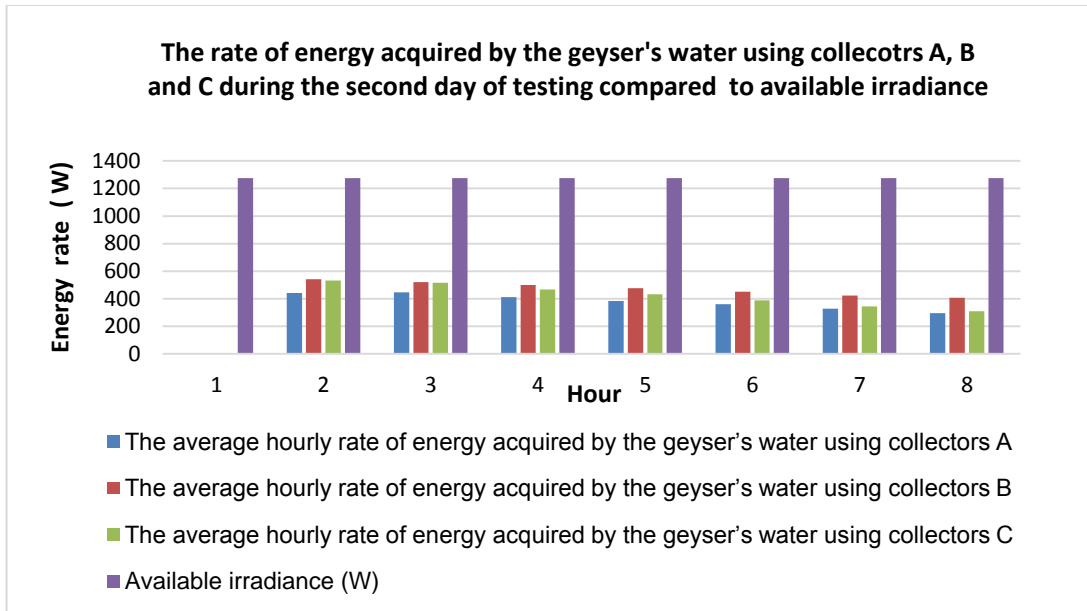


Figure 4.7: Comparison between energy acquired by the geyser's water using collectors A, B, and C relative to available irradiance during the second day of testing

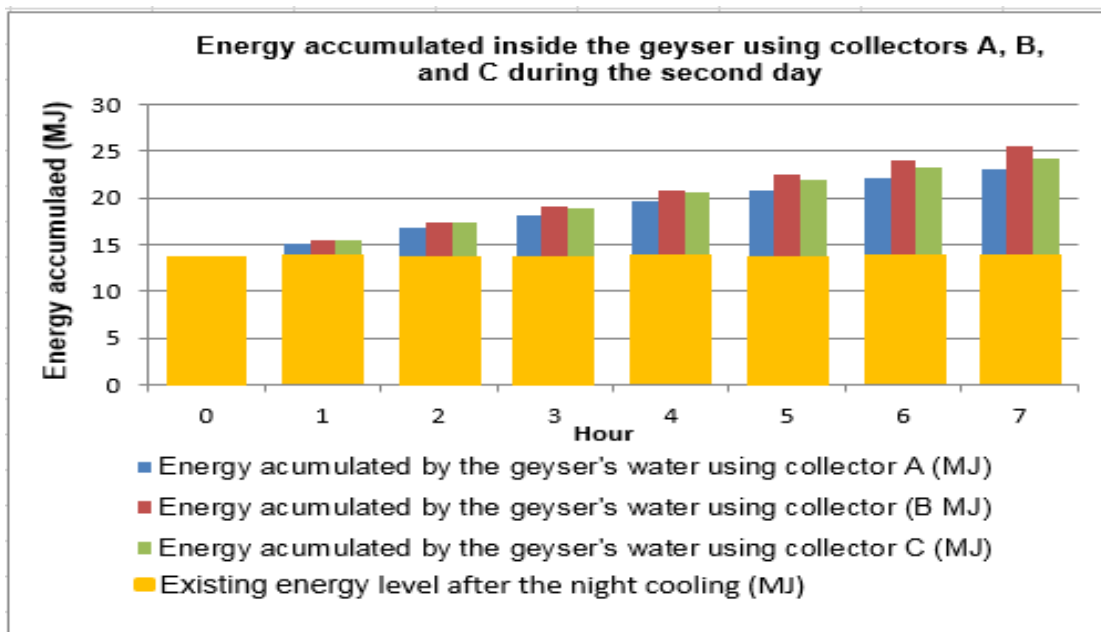


Figure 4.8: Comparison of cumulative energy delivered to the geyser from the flat plate solar collectors A, B, and C during the second day

4.4 Thermo-syphon solar water heating system's efficiency

The system's efficiency was calculated during the first day and the second day, as follows:

- **First day**

Following the results that appear in figure (4.5), it is easy to obtain hourly efficiencies for the water heating system as dependent on the performance of the three flat plate solar collectors A, B and C. The system's thermal efficiency is a simple ratio of the energy the panels were able to transfer to the water in the geyser compared to the irradiance available as shown figure (4.9). See appendix (D-1) for the calculation of hourly efficiency (%) using the collectors A, B, and C.

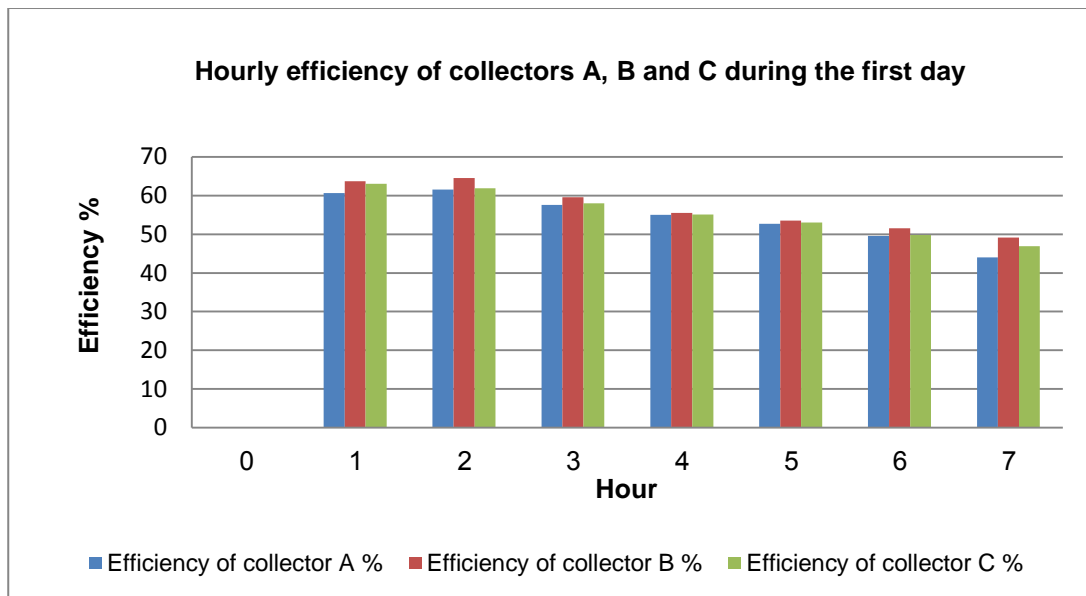


Figure 4.9: Hourly efficiency of the flat plate solar collectors A, B and C during the first day of the tests

- **Second day**

Similarly the thermal efficiency of the system for the second day of testing was obtained following the same procedure and the results are depicted in figure (4.10). See appendix (D-2) for the calculation of hourly efficiency (%) using the collectors A, B, and C.

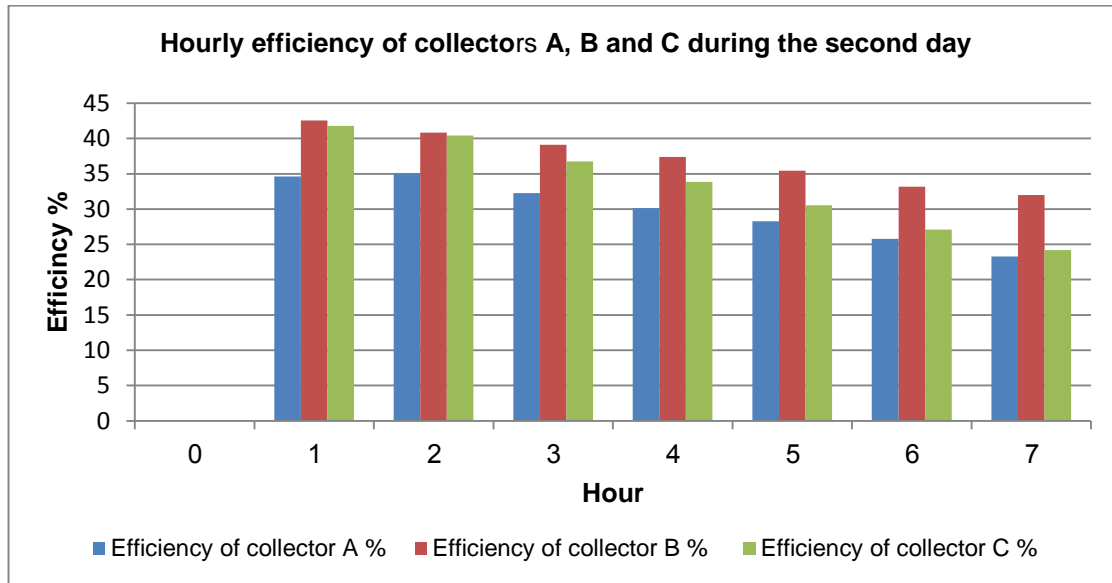


Figure 4.10: Hourly efficiency of the flat plate solar collectors A, B and C during the second day of the tests

4.5 Results from the dimensional analysis

The results obtained in chapter two and the experimental data from the collectors A, B and C for the period of the first day were used to obtain the functional relationship of the Π numbers. Π_2 and Π_3 were calculated for the collectors by using equations no (2.8) and (2.9), respectively. The pressure difference between the inlet and the outlet of the collectors A, B and C was calculated using equation (2.11), Π_1 was calculated using equation (2.7), as shown in Appendix (E). The average differences in pressure between the inlet and the outlet of the collectors A, B and C were 7908.9 (Pa), 6338.1(Pa) and 5162.6 (Pa) respectively. The average temperature of the water flowing inside the collectors was taken as the average of the outlet and inlet temperatures from the geyser and all properties (i.e. enthalpy and density) involved in the Π numbers were evaluated at this average temperature value (41.4°C) as shown in table (4.1).

Table (4.1): The values of Π_1 , Π_2 and Π_3 ; and the average pressure difference on the collectors A, B and C based on their vertical height

Collector	A	B	C
Vertical height L (m)	0.805	0.645	0.525
ΔP_{avg} (Pa)	71912.1	6337.2	5170.4
Π_1	1.0	1.0	1.0
Π_2	0.031091	0.034734	0.038499
Π_3	21955.29	27401.56	33664.77

It is to be noted that Π_1 is a constant having the value of unity therefore any functional relationship with Π_2 and Π_3 has to conform to either of the two possibilities from the results of the procedure shown below in figure (4.11) and (4.12), respectively:

Firstly, the relationships of Π_2 and Π_3 are obtained from the following graphs (figures 4.11 and 4.12), respectively.

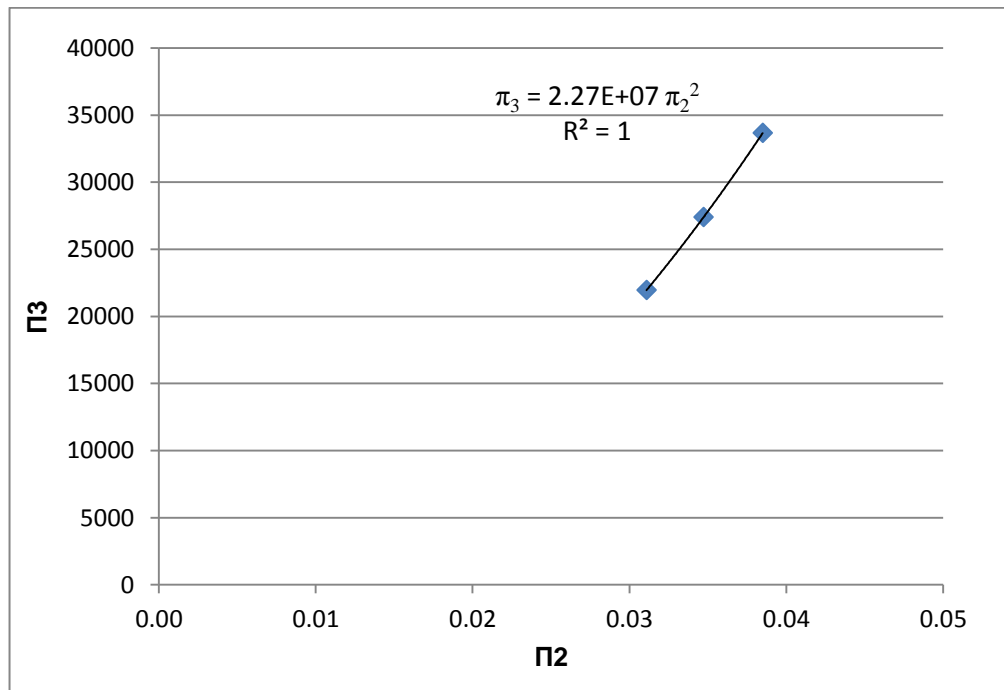


Figure 4.11: The relationship between Π_3 and Π_2

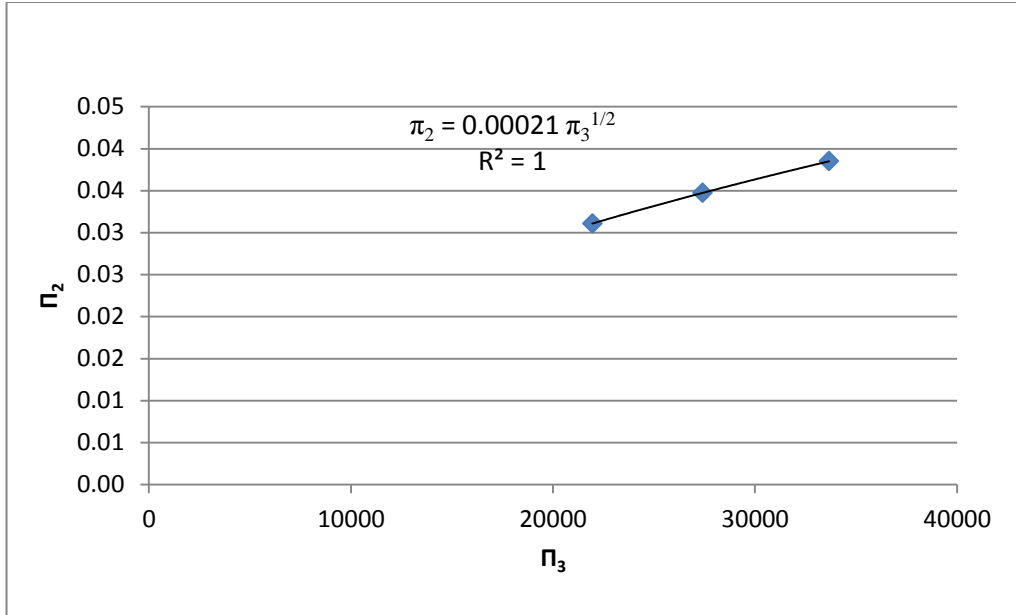


Figure 4.12: The relationship between Π_2 and Π_3

Therefore Π_1 can be formulated with either one of the expressions below:

$$\Pi_1 = \frac{\Pi_2}{(2.1 \times 10^{-4} * \Pi_3^{0.5})} = 1.0 \quad (4.1)$$

$$\Pi_1 = \frac{\Pi_3}{(2.27 \times 10^{-4} * \Pi_2^2)} = 1.0 \quad (4.2)$$

Expressions (4.1) or (4.2) may be useful to flat plate solar collector designers investigating the effect of changing one parameter to the remaining parameters in the dimensionless groups. For example the difference in pressure between the inlet and outlet of the flat plate solar collector can be calculated for any vertical height created by the inclined installation of the panel of the flat plate collector simply from Π_1 since it is a constant with the known value of unity as shown in figure (4.13)

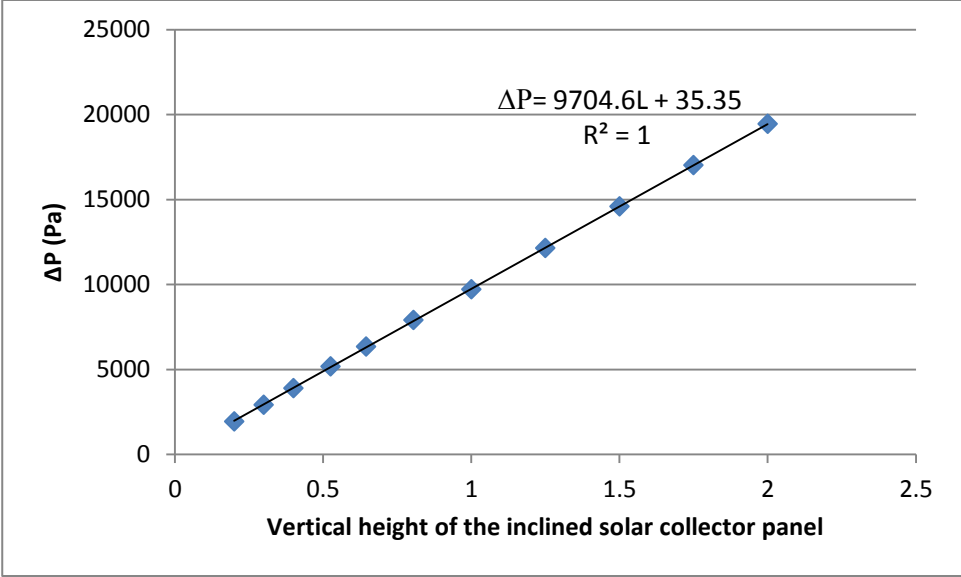


Figure 4.13: The difference in pressure between the inlet and outlet of the inclined solar collector panel vs. the vertical height between them

CHAPTER FIVE

Conclusions and Recommendations

5.1 Conclusions

The results were obtained from this study using three flat plate collectors A, B and C in a solar water heating system were considered or thought to be similar during the first day of the test, however there was a slight difference in the performance of these three collectors during the second day of the test. Hence the following conclusions were drawn:

5.1.1 Results from the first day of the tests

The results are summarised as follows:

- The water temperature increased gradually inside the geyser from the beginning of the test, ranging from 16.4 to 64.5°C using collector A, 16.4 to 66.5°C using collector B and 16.4 to 65.3°C using collector C. While the average temperature for the water inside the geyser using collectors A, B and C were 41.7°C, 42.7°C and 42.1°C, respectively.
- The rate of energy acquired or absorbed by the collectors A, B and C from what was available in terms of the irradiance from the solar spanned the range of 773.5 to 561.1 W, 812.2 to 626.9 W and 803.8 to 598.2 W, respectively.
- The total amount of heat delivered to the water inside the geyser by the collectors A, B and C during the first day of the testing period was 17.49 MJ, 18.24 MJ and 17.79 MJ respectively.
- Finally the calculation for the system's thermal efficiency when using collectors A, B and C during the first day spanned ranges from 60.6% to 44% , from 63.7% to 49.1% and from 63% to 46.9%, respectively.

5.1.2 Results from the second day of the tests

The results are summarised as follows:

- The average water temperature in the geyser was lowered during the overnight cooling period but of course increased gradually inside the geyser from the beginning of the second day of the test ranging from 53.6°C to 80°C using collector A, 53.6°C to 86.5°C using collector B and 53.6°C to 83.2°C using collector C. hence the average temperature

for the water inside the geyser using collectors A, B and C reached the levels of 67.7°C, 70.9°C and 69.8°C, respectively.

- The rate of energy acquired or absorbed by the collectors A, B and C from what was available in terms of the irradiance from the solar simulator spanned the range of 441.5 to 296.6 W, 542.6 to 407.8 W and 532.5 to 308.4 W respectively.
- The total amount of heat delivered to the water inside the geyser by the collectors A, B and C were 23.15 MJ, 25.49 MJ and 24.3 MJ, respectively.
- The system's thermal efficiency using the three collectors varied from 34.6% to 23.3 %, for collector A, from 42.5% to 32 % for collector B and, 41.7% to 24.2 % for collector C.

Therefore, the results obtained when experimenting with the flat plate solar collectors strongly rank solar collector B (of the 'square sides' geometrical configuration) as the best, followed by collector C (of the 'rectangle horizontal side long' configuration), and collector A (of the 'rectangle vertical side long' configuration) as the last one.

5.2 Results from the Dimensional Analysis

The experimental data applied to the dimensionless groups that were obtained from the dimensional analysis, yielded a functional equation which can be used as a tool in designing flat plate solar collectors.

$$\Pi_1 = \frac{\Pi_2}{(2.1 \times 10^{-4} * \Pi_3^{0.5})} = \frac{\Pi_3}{(2.27 \times 10^{-4} * \Pi_2^2)}$$

5.3 Recommendations for future work

- An investigation on the effect of the wind blowing on the surface of the flat plate collectors from all relevant directions could influenced their performance and hence affect the current arrived at ranking.
- A future work may attempt to redo the experiments using a pump driving a 'working fluid' through the solar collector in a closed loop with a heat exchanger inside the geyser.

REFERENCES

- [1] A Wadud, M.Zaman, F. Rabbee and R. Rahman, 'Renewable Energy : An Ideal Solution of energy crises and economic development in Bangladesh', *Global Journal*. 13.(15,2013),19-28.[October, 2015].
- [2] G, Jones and L,Bouamane."Power from Sunshine ": A Business History of Solar Energy. Internet: <http://www.hbs.edu/faculty/Publication%20Files/12-105.pdf>,May. 2005 [Oct, 2016].
- [3] H. Trollip, A. Butler, J. Burton, T. Caetano, and C. Godinho, "Energy security in South Africa," *Mitig. Action Plans Scenar*, Cape Town,2014.
- [4] V. Belessiotis and E. Delyannis (1999, November). "The history of renewable energies for water desalination," *Desalination*. [Online]. 128. 147–159. Available: www.elsevier.com/locate/desal [October,2014].
- [5] V. G. Belessiotis and E. Papanicolaou.(2012). "History of Solar Energy," *Comprehensive Renewable Energy*. 3. 85–102. Available: <http://www.elsevier.com/science/article/pii/B9780080878720003036>.
- [6] S. Wieder. *An Introduction to Solar Energy for Scientists and Engineers*. USA: John Wiley & Sons, Inc., 1982.
- [7] G. N. Tiwari. *Solar Energy: Fundamentals, Design, Modelling and Applications*. Alpha Science International, Limited, 2013.
- [8] R. Shukla, K. Sumathy, P. Erickson, and J. Gong.(2013). "Recent advances in the solar water heating systems: A review," *Renewable and Sustainable Energy Reviews*. [Online]. 19. 173–190. Available: www.elsevier.com/locate/rser [February, 2015].
- [9] J.A. Prajapati, J.K. Nayak. (2006, May). *Handbook On energy Conscious Buildings*. [Online] Available: <http://mnre.gov.in/solar-energy/ch2.pdf> [November, 2014].
- [10] J. Duffie and W. Beckman. *Solar Engineering Of Thermal Processes*. John Wiley & Sons, Inc. 2006.
- [11] P. P. Groumpos and K. Khouzam. "A generic approach to the shadow effect of large solar power systems." *Sol. Cells*. [online]. 22. (Sep.1987), pp. 29– 46. Available: <http://www.sciencedirect.com/science/article/pii/0379678787900688> [November, 2015].
- [12] Y. R. Sekhar, K. V Sharma, and M. B. Rao. (2009). "Evaluation of Heat Loss Coefficients in Solar flat plate collectores." [Online]. 4, (5) pp. 15–19. Available: www.arnjournals.com/jeas/research_papers/rp.../jeas_0709_208.pdf [January, 2015].
- [13] S.P, Sukhatme and Nayak, J.K. *Solar Energy: Principles of Thermal Collection and Storage*. New York: Tata McGraw-Hill, 2008.
- [14] S. K. Amrutkar, S. Ghodke, and K. N. Patil.(Feb,2012) "Solar Flat Plate Collector Analysis," *IOSR J. Eng.* [Online]. 2.(2), pp. 207–213. Available: www.iosrjen.org/Papers/vol2_issue2/F022207213.pdf [November, 2014].

- [15] W.B. Stine, R.W.Harrigan. (1986). Solar Energy Systems Design. [Online]. Available: www.powerfromthesun.net/Book/chapter06/chapter06.html [July, 2014].
- [16] D. M. Ghamari and R. A. Worth.(1992, February). "The effect of tube spacing on the cost-effectiveness of a flat-plate solar collector." *Renew. Energy* [Online]. 2. (6), pp. 603–606.Available: <http://www.sciencedirect.com/science/article/pii/096014819290025X> [Dec,2014].
- [17] M. O. Hamdan, H. A. N. Hejase, H. M. Noura, and A. A. Fardoun. (2014). ICREGA'14 - Renewable Energy: Generation and Applications. [Online].Available: <https://books.google.com/books?id=Rs4kBAAQBAJ&pgis=1> [May,2015].
- [18] L, Nathan S. "Basic Reserch Needs for Solar Energy Utilization:Report on the Basic Energy Sciences Workshop on Solar Energy Utilization" internet: http://science.energy.gov/~/media/bes/pdf/reports/files/seu_rpt.pdf [Jan, 2016].
- [19] W.B. Stine and M, Geyer. (2001). Power from the sun. [Online].Available: <http://www.powerfromthesun.net/Book/chapter02/chapter02.html> [August, 2014].
- [20] M, Pidwirn. (2006) "Atmospheric Effects on Incoming Solar Radiation" in *Fundamentals of Physical Geography*, 2nd Edition. [Online] Available :<http://www.physicalgeography.net/fundamentals/7f.html><http://www.physicalgeography.net/fundamentals/7f.html> [April,2016].
- [21] M.S.Hossain, R.Saidur,H.Fayaz,N.A.Rahim,M.R.Islam,J.U.Ahmed and M.M.Rahmn.(2011). "Review on solar water heater collector and thermal energy performance of cirulating pipe." *Renewableand Sustainable Energy Reviews*.[Online].15(2011), 3801-3812.Available: www.elsevier.com/locate/rser.
- [22] R, Plante. *Solar Domestic Hot Water: a practical guide to installation and understanding*. New York:Wiley,1983.
- [23] Y, Cengel, J, Cimbala and R, Turner. *Fundamentals of Thermal-Fluid Sciences* .New York: McGraw-Hill, 2012.
- [24] Y, Cengel. *Heat Transfer: a Practical Approach*.Boston: McGraw-Hill, 2003.
- [25] F, Incropera, D,Dewitt, T, Bergman and A, Lavine. *Fundamentals of Heat and Mass Transfer*. Hoboken, NJ: John Wiley, 2007.
- [26] R.W Fox; A.T. McDonald; Ph. J. Pritchard and J. C. Leylegian. *Fluid mechanics*. Hoboken, NJ : John Wiley, 2012.
- [27] R, Snieder. *A guided tour of Mathematical Methods for the Physical Sciences*. Cambridge; New York: Cambridge University Press, 2001.
- [28] N.P.Bansal, J.B.Singh, J.Lamon and S.R.choi. *Processing and Properties of Advanced Ceramics and Composites III*. Hoboken, NJ: John Wiley,2011.
- [29] "Application of Buckingham Pi theorem." Internet: <http://www-mdp.eng.cam.ac.uk/web/>

- library/enginfo/aerothermal_dvd_only/aero/fprops/dimension/node9.html, 2005.
[Jan,2016].
- [30] "Solar max". Internet: <http://www.solarmax.co.za/products/solar-geysers/> [20 Nov, 2015].
- [31] "Solar max". Internet: <http://www.solarmax.co.za/products/smx-solar-collectors/> [23 Nov, 2015].
- [32] "WeiKu.com". Internet: http://www.weiku.com/products/9158154/laser_pex_al_pex_for_hot_water.html [16 November, 2015].
- [33] "TES insterment". Internet: <http://www.tes-meter.com/tes1333.htm> [16 March, 2015].
- [34] "Unitempm".Internet: <http://www.unitemp.com/search/node/testo%20926> [April, 2015].
- [35] "DEWEsoft".Internet: <http://www.dewesoft.com/pro/course/temperature-measurement-2> [April, 2015].
- [36] "PraguyNacorn". Internet: <http://www.praguynakorn.com/product/3/sb-10> [Feb,2016].
- [37] "Tes insturment". Internet: <http://www.tes-meter.com/tes1333.htm> [Feb,2016]

APPENDICES

Appendix A: Technical specification of experimental instrumentation

Appendix A-1: Variable voltage transformer-Variac model: SB-10 and specifications



Figure A-1: Variable voltage transformer-Variac model: SB-10
(Adopted from [36])


Table A-1: specification of Variable voltage transformer-Variac model: SB-10 and specifications
(Adopted from [36])

Max. Current	Capacity	Mount	Dimension H x Ø	Net (Weight)
10 A	2 KVA	5	156 X 235 mm	11 Kg.

Appendix A-2: Solar power meter (TES-1333) specifications
 (adopted from [37])

Display	3-1/2 digits. Max. indication 1999
Range	2000 W/m ² 、634 Btu/(ft ² * h)
Resolution	1W/m ² 、1Btu/(ft ² *h)
Spectral response	400-1100 nm
Accuracy	Typically within ± 10 W/m ² [± 3 Btu / (ft ² *h)] or $\pm 5\%$, whichever is greater in sunlight; Additional temperature induced error ± 0.38 W/m ² / °C [± 0.12 Btu / (ft ² *h)/ °C] from 25 °C
Angular accuracy	Cosine corrected <5% for angles <60 °
Drift	< $\pm 2\%$ / per year
Calibration	User recalibration available
Over-input	Display shows
Sampling Time	Approx. 0.4 second
Manu data memory and read	99 sets
Auto data memory	32000 sets (TES-1333R)
Battery	4pcs size AAA
Battery Life	Approx. 100 hours
Operating temp and humidity	0 °C to 50 °C below 80%RH
Storage temp and Humidity	-10 °C to 60 °C below 70% RH
Weight	Approx. 165 g
Dimension	111(L)*64(W)*34(H)mm
Accessories	Carrying Case, Operation Manual, 4 pcs size AAA, RS232 cable(for TES-1333R), CD software (For TES-1333R)

Appendix A-3: T-type thermocouple quality inspection certificate

	7 Vuursig Avenue Spartan Ext 7, Kempton Park 1619 T: 011 966 8600 F: 011 392 5235	Temperature Sensor Quality Inspection Certificate
	47 Flamingo Crescent, Lansdown, Cape Town, 7779 T: 021 7628995 F: 021 762 8996	

Temperature Sensor - Quality Inspection Certificate

Customer: CPUT
 Job Number: C317853 A
 Drawing/Part No: STY 020441
 Date of Inspection: 2/4/15

Order Quantity		Quantity to inspect
From	To	
1	3	All (100%)
5	10	3 off
10	50	6 off
50	100	10 off
100 +	100	15 off

	NOMINAL		ACTUAL	
Sensor type, class:	T			
Stem Length L1, L2 (mm):	L1:	L2:	L1:	L2:
Stem Diameter D1, D2 (mm):	D1:	D2:	D1:	D2:
Termination Type:				
Mounting Type:				
Cable Option:	Teflon			
Cable Length:	200mm		200mm	
Grounded or Ungrounded:	E			

Sample No.	Tolerance Spec. #	Calibrator Temp.	Sample Temp.	Variance	Accepted?
1	-20.13 TS.13	98.51	99.09	-0.58	✓
2	"	98.49	98.63	-0.14	✓
3	"	98.50	97.8	0.7	✓
4	"	98.47	97.9	0.57	✓
5	"	98.51	99.15	-0.64	✓


- Are all weld seams in a good condition?
- Are there any mechanical defects on the sensor?
- Is the colour coding & polarity according to Sensor Ref. chart (U-IMS-MFR-DF-007)?
- Have the label details been checked and are they acceptable?
- Do the sensor response times correspond with the Tolerance Reference Chart*?
- Is the insulation of ungrounded sensors higher than 1000mΩ at 100V?
- Is the jobcard and drawing (if applicable) updated and correct?

<input checked="" type="checkbox"/>	YES	<input checked="" type="checkbox"/>	NO
<input checked="" type="checkbox"/>	YES	<input checked="" type="checkbox"/>	NO
<input checked="" type="checkbox"/>	YES	<input checked="" type="checkbox"/>	NO
<input checked="" type="checkbox"/>	YES	<input checked="" type="checkbox"/>	NO
<input checked="" type="checkbox"/>	YES	<input checked="" type="checkbox"/>	NO
<input checked="" type="checkbox"/>	YES	<input checked="" type="checkbox"/>	NO

* Refers to Tolerance Reference Chart- Sensors U-IMS-MFR-D-003 Rev 03

Remarks

The above sensors were found: Acceptable Rejected

QA Inspector: skw Signed:  Date: 2/4/15

Appendix A-4: Testo 926 digital thermometer certificate of conformity and digital technical data

		Kalibrier-Protokoll Certificate of conformity • Protocole d'étalonnage Protocollo di collaudo • Informe de calibración
Gerät / Module type / Modèle / Modelo:		testo 926
Meßbereich / Measuring range / Etendue de mesure / Rango de medición:		-50...+400°C
Serien-Nr. / Serial no. / No. de série / Número de serie:		33835720
Segmenttest / Display test / Test d'affichage / Test del visualizador:		<input checked="" type="checkbox"/> OK
Meßwerte / Measured values / Valeurs mesurées / Valores medidos:		
Sollwert / Reference / Référence / Referencia:		Istwert / Actual Value / Valeur réelle / Valor medido:
+80.0 °C		+79.9 °C
		
Prüfer / Inspector / Responsable / Verificador		

9. Technical data

Characteristic	Value
Parameters	Temperature (°C/°F / °R)
Measuring range	-50.0...+400 °C / -58.0...+752.0 °F / -40.0...+320 °R
Resolution	0.1 °C / 0.1 °F / 0.1 °R (-50.0...+199.9 °C / -58.0...+391.8 °F / -40.0...+159.9 °R) 1 °C / 1 °F / 1 °R (rest of range)
Accuracy (± 1 Digit)	±0.3 °C / ±0.6 °F / ±0.2 °R (-20.0...+70.0 °C / -4.0...+158.0 °F / -16.0 ... +56.0 °R) ±0.7 °C+0,5% o.r. / ±1.3 °F+0,5% o.r. / ±0.6 °R + 0,5% o.r. (rest of range)
Probe connections	1x Omega TC socket for temperature probe type T (Cu-CuNi), radio module (accessory part)
Measuring rate	2/s
Operating temperature range	-20 ... +50 °C / -4 ... +122 °F / -16 ... +40 °R
Storage temperature	-40 ... +70 °C / -40 ... +158 °F / -32 ... +56 °R
Voltage supply	1x 9 V monobloc battery/rech. battery
Running time (display lighting off / on)	with probe connected: approx. 200 h / approx. 68 h, with radio probe: approx. 45 h / 33 h
Protection class	with TopSafe (accessory part) and probe connected: IP65
EC Directive	2004/108/EC
Warranty	2 years, warranty conditions: see www.testo.com/warranty

With TopSafe and the following probes, this product complies with guidelines in accordance with the EN 13485 standard:

Part no.	Measuring range
0613 1001	-50...+275 °C / -58.0...+527 °F
0603 1293	-50...+350 °C / -58.0...+662 °F
0603 1793	-50...+350 °C / -58.0...+662 °F
0603 2192	-50...+350 °C / -58.0...+662 °F
0603 2492	-50...+350 °C / -58.0...+662 °F
0603 3292	-50...+350 °C / -58.0...+662 °F

Suitability: S, T (storage, transport)
Environment: E (transportable thermometer)
Accuracy class: 0.5
Measurement range: see table above

According to EN 13485, the measuring instruments should be checked and calibrated regularly under the terms of EN 13486 (Recommended: Yearly).
Contact us for more information: www.testo.com

Appendix B: Temperatures during the test period

Table B-1: Temperatures inside the geyser (in different locations) during the test period of the first day using collectors A, B, and C

Time (hour)	T ₁ (°C)	T ₂ (°C)	T ₃ (°C)	T ₄ (°C)	T ₅ (°C)	T ₆ (°C)	T _{avg} (°C)
Flat Plate Solar Collector A							
0	16.7	16.5	16.5	16.2	16.4	16.1	16.4
1	31.5	29.4	26.2	21.8	18.2	17.2	24.1
2	44.1	41.4	35.4	28.4	22.6	19	31.8
3	55	51	44.4	35.4	27.4	21.3	39.1
4	65.1	60	52.5	42.6	32.1	23.8	46.0
5	74	67.9	60.6	49.6	37	26.9	52.7
6	81	74.5	68.3	56.4	42.3	31	58.9
7	85	81	74.5	62.9	47.4	36	64.5
Flat Plate Solar Collector B							
0	16.7	16.5	16.4	16.4	16.3	16.1	16.4
1	33.4	28.9	26.3	22	19	17	24.4
2	48	40	35.5	29.7	22.9	19.3	32.6
3	58.5	50	44.4	37	27.8	22.8	40.1
4	67.5	58	52.6	44.5	33	26.9	47.1
5	74	65.7	60.7	51.6	39	32	53.8
6	78.8	72.7	68	59.7	45	37.8	60.3
7	83	78.4	74.5	68.3	51	44	66.5
Flat Plate Solar Collector C							
0	16.7	16.6	16.4	15.9	16.5	16.4	16.4
1	32.7	28.6	25.1	23.1	18.5	18.2	24.4
2	47	39.7	34	30.5	21.1	20.7	32.2
3	58	49.8	43.1	37.9	24.6	23.5	39.5
4	67.6	57.8	51.7	45.5	30	26	46.4
5	75.1	65.4	60	52.8	35.8	29.6	53.1
6	80.8	71.7	67.1	60.6	42.3	33.9	59.4
7	84.7	77	73	68.8	49.9	38.5	65.3

Table B-2: Temperatures inside the geyser (in different locations) during the test period of the second day using collectors A, B, and C and C

Time (hour)	T ₁ (°C)	T ₂ (°C)	T ₃ (°C)	T ₄ (°C)	T ₅ (°C)	T ₆ (°C)	T _{avg} (°C)
Flat Plate Solar Collector A							
0	61.1	60.2	59	54.2	45.2	41.8	53.6
1	67	65.3	64	59.6	49.1	42.7	58.0
2	74	70.4	68.5	63.9	53.4	44	62.4
3	79.3	75.3	72.6	68.3	56.8	46.3	66.4
4	83.5	78.9	76.7	72.5	60.4	49.4	70.2
5	87	82.4	80.1	76.3	63.9	53.1	73.8
6	90.5	85.2	82.5	78.9	67.5	57.7	77.1
7	92.5	87.8	85.2	81.8	70.7	61.9	80.0
Flat Plate Solar Collector B							
0	63.1	57.7	56.8	52.2	46.7	45.3	53.6
1	70.7	65.4	63	58.2	49.6	47.1	59.0
2	76.9	71.5	69	64	53.2	50.3	64.2
3	82.5	76.2	74.2	69.8	57.8	54	69.1
4	87.5	81	78.8	74.8	62.5	58.2	73.8
5	91.5	85.4	83.4	79.6	67	62.7	78.3
6	94.1	90.1	87.8	83.7	71.8	67.2	82.5
7	96.4	93.6	91.6	87.6	77.8	71.9	86.5
Flat Plate Solar Collector C							
0	68.8	58.7	57.7	54.4	43.8	38.5	53.7
1	73.1	66.7	63.9	60	48.4	41.4	58.9
2	77.7	72.5	70.3	66.2	52.5	44.9	64.0
3	81.9	77.8	75	71.9	56.6	48.7	68.7
4	85.1	82.6	80.2	76.6	60.5	52.5	72.9
5	89.7	85.9	83.9	80	65	56.1	76.8
6	92	89	87.2	84.3	68.6	60	80.2
7	95.7	91.2	90	87	71.9	63.6	83.2

Appendix C: Sample calculations

Appendix C-1: Sample of the experiment calculations

- **Input**

The amount of the input heat was calculated using equation (2.4):

$$\begin{aligned} Q_i &= I \cdot A & (2.4) \\ &= 850 \times 1.5 = 1275 \text{ W} \end{aligned}$$

Where: Q_i is the heat input to the collector (W), I is intensity of solar radiation W/m^2 , A is the collector's surface area exposed to the sun's irradiance m^2 .

- **Sample calculation of the energy rate acquired by the geyser's water**

The energy rate acquired by the geyser's water was calculated using equation (2.5):

$$Q_o = \frac{m_g C_p \Delta T_{avg}}{\Delta t} \quad (2.5)$$

Where Q_o is the energy rate acquired by the water in the geyser (W), m_g is the mass inside the geyser (kg) equivalent to the 88 litres, at an average density 988.1 kg/m^3 , ΔT_{avg} is the average temperature inside the geyser recorded (i.e. average of six temperatures inside the geyser) ($^{\circ}\text{C}$) during Δt which is the time interval of data collection, i.e. an hour = 3600 seconds. C_p is the average specific heat of the water (4186) Joules/kg $^{\circ}\text{C}$.

The calculation for the heat acquired by the water in the geyser shown here is for the first day of the test using collector A at the third hour when the average water temperature increased from 31.8°C to 39.1°C .

$$Q_o = 86.95 \times 4186 \times (39.1 - 31.8) / 3600 = 735 \text{ W}$$

- **Sample calculation of the energy accumulated by the geyser's water (MJ)**

The energy accumulated by the geyser's water for the first day of the test using collector A at the third hour when the average water temperature in the beginning of the test 16.4°C increased to 39.1°C was calculated using the following equation:

$$Q_{ac} = m_g C_p \Delta T_{avg} = 86.95 \times 4186 \times (39.1 - 16.4) = 8.256 \text{ MJ}$$

- **Sample calculation of the hourly efficiency (%)**

The system's hourly efficiency was calculated using equation (2.6):

$$\text{Efficiency} = \frac{\text{Energy rate acquired}}{\text{Energy Input}} \times 100 \quad (2.6)$$

$$= 735 \text{ W}/1275 \text{ W} \times 100 = 57.64 \%$$

Appendix C-2: The difference in pressure between the inlet and outlet of the flat plate collector

The pressure difference between the inlet and outlet of the collector was calculated for the first day of the test using collector A at the third hour when the average water temperature was 38.2°C, the inlet water temperature was 21.3°C and the outlet water temperature was 55°C, using equation (2.11):

$$P_i - P_o = [\rho_{avg} x_1 + \rho_{cold} x_2]g - [x_1 + x_3]g\rho_{hot} \quad (2.11)$$

$$\Delta p = (992.926*0.37+998.014*0.84)*9.81-(0.405)*9.81*985.65=7912 \text{ Pa}$$

Where P_i is the pressure at the inlet, P_o is the pressure at the outlet, ρ_{avg} (kg/m^3) is the density at the average temperature between the inlet and the outlet of the collector, ρ_{cold} (kg/m^3) is the density at the inlet ρ_{hot} (kg/m^3) is the density at the outlet temperature, x_1 , x_2 , x_3 are the relative vertical heights (m), g is earth's gravity (m/s^2).

Appendix C-3: Sample calculation of the Π (dimensionless) numbers

The three dimensionless numbers for example are calculated using data from the first day of the test of the flat plate solar collector A (at the third hour) when the average water temperature was 38.2°C:

- $\Pi_1 = \frac{\Delta p}{L \rho g}$

$$\Pi_1 = \frac{7912 \text{ (Kg/ms}^2\text{)}}{0.805 \text{ (m)} \times 992.926 \text{ (Kg/m}^3\text{)} \times 9.81 \text{ (m/s}^2\text{)}} = 1$$

- $\Pi_2 = \frac{I}{\rho L^{1/2} g^{3/2}}$

$$\Pi_2 = \frac{850 \text{ (W/m}^2\text{)}}{992.926 \left(\frac{\text{kg}}{\text{m}^3}\right) \times 9.81 \text{E}1.5 \left(\frac{\text{m}}{\text{s}^2}\right) \times 0.805 \text{E}0.5 \text{ (m)}} = 0.03105$$

- $\Pi_3 = \frac{h}{L g}$

$$\Pi_3 = \frac{160.016 \left(\frac{\text{KJ}}{\text{Kg}}\right) \times 1000}{9.81 \left(\frac{\text{m}}{\text{s}^2}\right) \times 0.805 \text{ m}} = 20262.76$$

Where: Δp is the pressure difference between inlet and outlet of the solar collector (Pa), ρ is the density of the water (kg/m^3), g is earth's gravity (m/s^2), L is the vertical height difference between input (cold water) and output (hot water) of the collector (m), I is the amount of solar radiation incident on the collector's surface (W/m^2) and h is the water's specific enthalpy flowing in the collector (Joule/kg).

Appendix D: The calculation of energy rate acquired, energy accumulated by the geyser's water and hourly efficiency

Table D-1: T_{avg} ($^{\circ}\text{C}$), ΔT , energy rate acquired by the geyser's water (W), energy accumulated by the geyser's water (MJ) and hourly efficiency (%) were calculated during the test period of the first day using the collectors A, B, and C

Time (hour)	T_{avg} ($^{\circ}\text{C}$)	ΔT ($^{\circ}\text{C}$)	Energy acquired by the geyser's water (W)	Energy accumulated by the geyser's water (MJ)	Hourly efficiency (%)
Using Flat Plate Solar Collector A					
0	16.4	0	0	0	0.00
1	24.1	7.65	773.47	2.784480819	60.66
2	31.8	7.77	785.26	5.611426487	61.59
3	39.1	7.27	734.71	8.256379945	57.62
4	46.0	6.93	701.01	10.78000526	54.98
5	52.7	6.65	672.36	13.20050166	52.73
6	58.9	6.25	631.92	15.47540429	49.56
7	64.5	5.55	561.14	17.49551783	44.01
Using Flat Plate Solar Collector B					
0	16.4	0	0.00	0	0.00
1	24.4	8.03	812.22	2.92400818	63.70
2	32.6	8.13	822.34	5.884414803	64.50
3	40.1	7.52	759.99	8.620364366	59.61
4	47.1	7.00	707.75	11.16825531	55.51
5	53.8	6.75	682.47	13.62515015	53.53
6	60.3	6.50	657.19	15.99104889	51.54
7	66.5	6.20	626.86	18.2477523	49.17
Using Flat Plate Solar Collector C					
0	16.4	0	0.00	0	0.00
1	24.4	7.95	803.80	2.893676145	63.04
2	32.2	7.80	788.63	5.732754628	61.85
3	39.5	7.32	739.76	8.395907306	58.02
4	46.4	6.95	702.69	10.92559903	55.11
5	53.1	6.68	675.73	13.35822824	53.00
6	59.4	6.28	635.29	15.64526369	49.83
7	65.3	5.92	598.22	17.79883818	46.92

Table D-2: T_{avg} ($^{\circ}\text{C}$), ΔT , Energy rate acquired by the geyser's water (W), Energy accumulated by the geyser's water (MJ) and Hourly efficiency (%) were calculated during the test period of the second day using the flat plate solar collectors A, B, and C

Time (hour)	T_{avg}	ΔT ($^{\circ}\text{C}$)	Energy acquired by the geyser's water (W)	Energy accumulated by the geyser's water (MJ)	Hourly efficiency (%)
Using Flat Plate Solar Collector A					
0	53.6	0.0	0.00	13.54	0.00
1	58.0	4.4	441.50	15.13083192	34.63
2	62.4	4.4	446.55	16.73842978	35.02
3	66.4	4.1	411.17	18.21863309	32.25
4	70.2	3.8	384.21	19.60177389	30.13
5	73.8	3.6	360.61	20.89998499	28.28
6	77.1	3.3	328.60	22.08293436	25.77
7	80.0	2.9	296.58	23.15062199	23.26
Using Flat Plate Solar Collector B					
0	53.6	0.0	0.00	13.54	0.00
1	59.0	5.4	542.61	15.49481634	42.56
2	64.2	5.2	520.70	17.36933611	40.84
3	69.1	4.9	498.79	19.16499258	39.12
4	73.8	4.7	476.89	20.88178577	37.40
5	78.3	4.5	451.61	22.50758285	35.42
6	82.5	4.2	422.96	24.03025101	33.17
7	86.5	4.0	407.80	25.4983215	31.98
Using Flat Plate Solar Collector C					
0	53.7	0.0	0.00	13.54	0.00
1	58.9	5.3	532.50	15.45720462	41.76
2	64.0	5.1	515.64	17.31352516	40.44
3	68.7	4.6	468.46	18.99998631	36.74
4	72.9	4.3	431.39	20.55298651	33.83
5	76.8	3.8	389.26	21.95432653	30.53
6	80.2	3.4	345.45	23.19793997	27.09
7	83.2	3.1	308.38	24.30809245	24.19

Appendix E: Temperature data, density values, enthalpy, pressure difference between the inlet and outlet of the flat plate collectors A, B and C and (Π_1 , Π_2 and Π_3)

Time (hr)	T_{avg} ($^{\circ}C$)	ρ_{avg} (kg/m^3)	ρ_{hot} (kg/m^3)	ρ_{cold} (kg/m^3)	h (KJ/kg)	ΔP (pa)	Π_1	Π_2	Π_3
Using collector A									
0	16.4								
1	24.4	997.28	995.25	998.824	102.352	7896.358	1.0	0.03092	12960.79
2	31.6	995.218	990.598	998.49	128.258	7904.604	1.0	0.03098	16241.25
3	38.2	992.926	985.65	998.014	160.016	7912.021	1.0	0.03105	20262.76
4	44.5	990.43	980.395	997.428	186.34	7919.011	1.0	0.03113	23596.15
5	50.5	987.79	975.28	996.644	211.42	7923.290	1.0	0.03121	26772.02
6	56.0	985.16	970.97	995.41	234.42	7920.699	1.0	0.03130	29684.50
7	60.5	982.865	968.39	993.73	253.25	7908.776	1.0	0.03137	32068.94
Using collector B									
0	16.4								
1	25.2	997.076	994.747	998.86	105.696	6330.103	1.0	0.03455	16704.360
2	33.7	994.529	988.920	998.43	141.216	6341.140	1.0	0.03464	22317.995
3	40.7	991.58	983.900	997.668	170.459	6345.298	1.0	0.03474	26939.604
4	47.2	989.272	979.060	996.617	197.626	6349.139	1.0	0.03482	31233.119
5	53.0	986.62	975.280	995.09	221.88	6344.345	1.0	0.03491	35066.259
6	58.3	984.004	972.354	993.074	244.044	6333.026	1.0	0.03501	38569.092
7	63.5	981.27	969.690	990.64	265.81	6317.450	1.0	0.03510	42009.024
Using collector C									
0	16.6								
1	25.6	996.968	994.859	998.585	107.368	5151.897	1.0	0.03830	20847.143
2	33.9	994.463	989.36	998.143	142.052	5162.224	1.0	0.03839	27581.574
3	40.8	991.938	984.16	997.5	170.876	5170.186	1.0	0.03849	33178.195
4	46.8	989.448	979.004	996.86	195.954	5178.118	1.0	0.03859	38047.473
5	52.4	986.902	974.62	995.834	219.366	5180.658	1.0	0.03869	42593.272
6	57.4	984.46	971.096	994.463	240.282	5178.263	1.0	0.03878	46654.434
7	61.6	982.282	968.585	992.815	257.854	5171.281	1.0	0.03887	50066.307